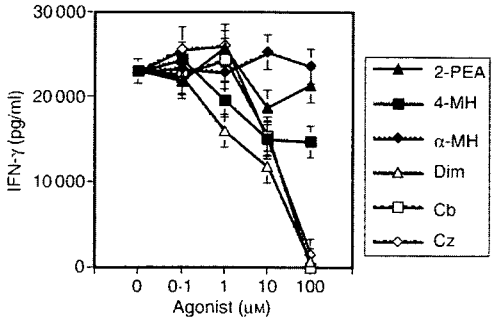

Figure 2. Inhibition of purified protein derivative of *Mycobacterium tuberculosis* (PPD)-induced interferon-γ (IFN-γ) production from peripheral blood mononuclear cells (PBMCs) by histamine receptor (HR)-selective agonists. PBMCs were cultured with 2 μg/ml of PPD in the presence or absence of serial dilutions of HR-selective agonists. Cb, clobenpropit; Cz, clozapine; Dim, dimaprit; 4-MH, 4-methylhistamine; α-MH, alpha-methylhistamine; 2-PEA, 2-pyridylethylamine. Results are expressed as the mean concentrations ± standard deviation (SD) from triplicate cultures. Data are representative of four separate experiments.

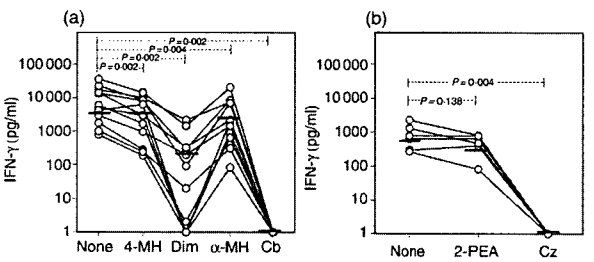

Figure 3. Inhibition of purified protein derivative of *Mycobacterium tuberculosis* (PPD)-induced interferon-γ (IFN-γ) production by histamine receptor (HR)-selective agonists. Peripheral blood mononuclear cells (PBMCs) were stimulated with PPD in the presence or absence of 100 μM HR-selective agonists. (a) Effect of 4-methylhistamine (4-MH), alpha-methylhistamine (α-MH), dimaprit (Dim) and clobenpropit (Cb) on PPD-induced IFN-γ production (n = 12). (b) Effect of 2-pyridylethylamine (2-PEA) and clozapine (Cz) on PPD-induced IFN-γ production (n = 6). The P-values were obtained using Wilcoxon's signed-rank test. Vertical bars represent the mean concentrations for each group.

dimaprit, clobenpropit and clozapine, inhibited PPD-induced IFN-γ production in a dose-dependent manner (Fig. 2). Complete inhibition of PPD-induced IFN-γ production was observed in the presence of 100 μM dimaprit (97·4 ± 3·8% inhibition; P = 0·002), clobenpropit (100% inhibition; P = 0·002), or clozapine (100% inhibition; P = 0·004). In contrast, 100 μM 2-PEA did not cause significant inhibition (33·4 ± 47·2% inhibition; P = 0·138) of PPD-induced IFN-γ production, and partial inhibition was observed using 100 μM 4-MH (63·6 ± 16·5% inhibition; P = 0·002) and α-MH (50·3 ± 35·0% inhibition; P = 0·004) (Fig. 3). None of the HR-related agonists

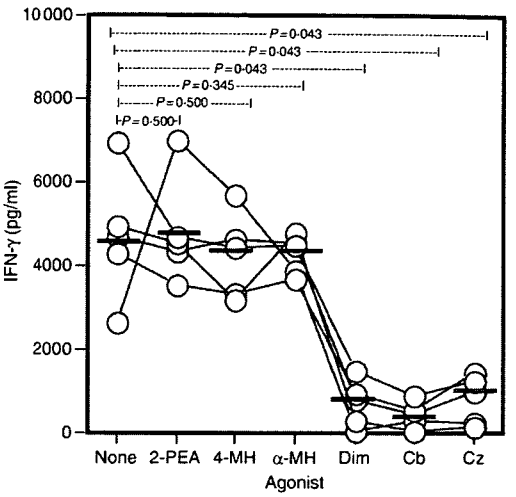

Figure 4. Histamine receptor (HR)-selective agonists-mediated inhibition of purified protein derivative of *Mycobacterium tuberculosis* (PPD)-induced interferon-γ (IFN-γ) production by T-cell lines (TCLs). Five PPD-specific TCLs were mixed with antigen-presenting cells (APCs) and cultured with 2 μg/ml of PPD for 65 hr in the presence of 100 μM 2-pyridylethylamine (2-PEA), 4-methylhistamine (4-MH), alpha-methylhistamine (α-MH), dimaprit (Dim), clobenpropit (Cb) and clozapine (Cz). Following incubation, supernatant was collected and the IFN-γ concentration of each sample was determined by enzyme-linked immunosorbent assay (ELISA). P-values were determined using Wilcoxon's signed-rank test. Data on each TCL are representative of two separate experiments.

induced IL-10 production in PPD-stimulated PBMCs (data not shown).

Similar results were seen when we used PPD-specific TCLs, the more purified cell populations. We generated five PPD-specific TCLs from five donors. Treatment with 2-PEA, 4-MH and α-MH did not affect the PPD-specific IFN-γ production. However, treatment with dimaprit, clozapine and clobenpropit strongly and dose-dependently inhibited these responses (Fig. 4).

Effect of HR-selective antagonists on the inhibition of IFN-γ production by H4R-selective agonists

To verify that the H4R-selective agonists inhibit PPD-specific IFN-γ production via H4R, we examined the influence of a panel of HR-specific antagonists. Addition of thioperamide, an antagonist of both H4R and H3R, did not reverse the inhibition of PPD-induced IFN-γ production by either histamine or H4R agonists (Fig. 5a). Furthermore, a mixture of *d*-chlorpheniramine, famotidine and thioperamide did not reverse the inhibition (Fig. 5b). These results were seen in both high responders (IFN-γ production > 10 000 pg/ml) and low responders (IFN-γ production < 10 000 pg/ml) for PPD-induced IFN-γ production (data not shown).

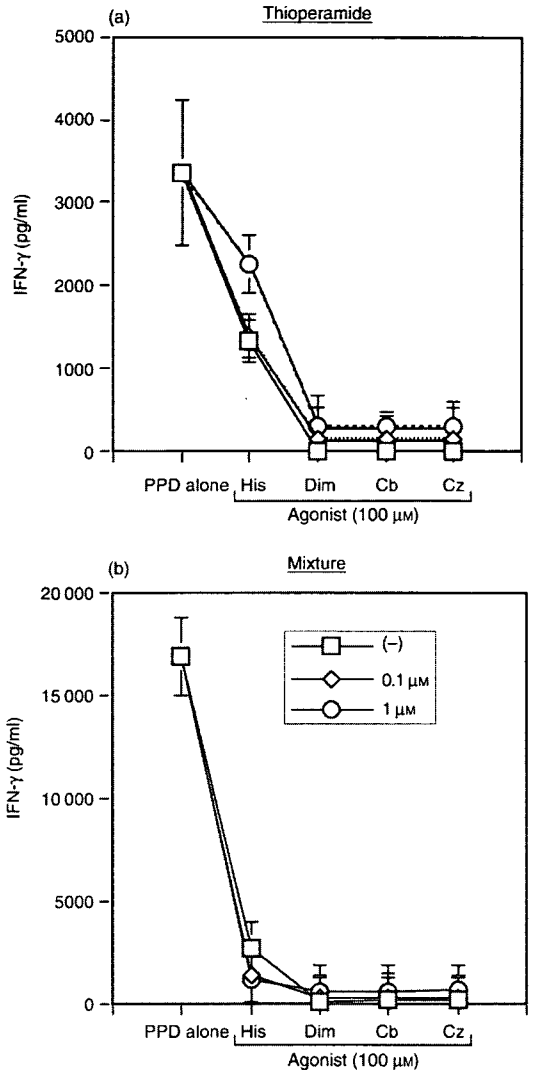

Figure 5. Effect of histamine receptor (HR)-selective antagonists on the inhibition of interferon-γ (IFN-γ) production induced by H4R-selective agonists. Peripheral blood mononuclear cells (PBMCs) were pretreated for 30 min with thioperamide (a) or with a mixture of antagonists (b) at the following concentrations: (a) pretreatment with 0 μM (square), 0·1 μM (diamond) or 1·0 μM (circle) thioperamide; (b) simultaneous pretreatment with each concentration of 0 μM (square), 0·1 μM (diamond) or 1·0 μM (circle) *d*-chlropheniramine, famotidine and thioperamide. Then, cells were incubated with 2 μg/ml of purified protein derivative of *Mycobacterium tuberculosis* (PPD) and 100 μM histamine (His), dimaprit (Dim), clobenpropit (Cb), or clozapine (Cz). Results are presented as the mean concentrations ± standard deviation (SD) from triplicate cultures. Data are representative of three separate experiments.

Role of adenylate cyclase and apoptosis in histamine suppression of PPD-induced IFN-γ production

We examined whether the inhibition by histamine and H4R-selective agonists depends on the activity of adenylate cyclase. Pretreatment of PBMCs with SQ22536, an adenylate cyclase inhibitor, reversed the inhibition of PPD-induced IFN-γ production by histamine and dimaprit. Furthermore, pretreatment with RP-8-Br-cAMPS, a PKA type 1 inhibitor, completely reversed the inhibition by histamine and dimaprit (Fig. 6a,b). Pretreatment of PBMC with SQ22536 and RP-8-Br-cAMPS also reversed the inhibition by clozapine (Fig. 6d), but the effects were weaker than observed for the reversal of inhibition by histamine. However, a minimal effect of SQ22536 and RP-8-Br-cAMPS was seen on the effect of clopenpropit (Fig. 6c). These results were seen in both high and low responders for PPD-induced IFN-γ production (data not shown). The addition of SQ22536 or RP-8-Br-cAMPS had no effect on the IFN-γ production by PBMCs in response to PPD alone (data not shown).

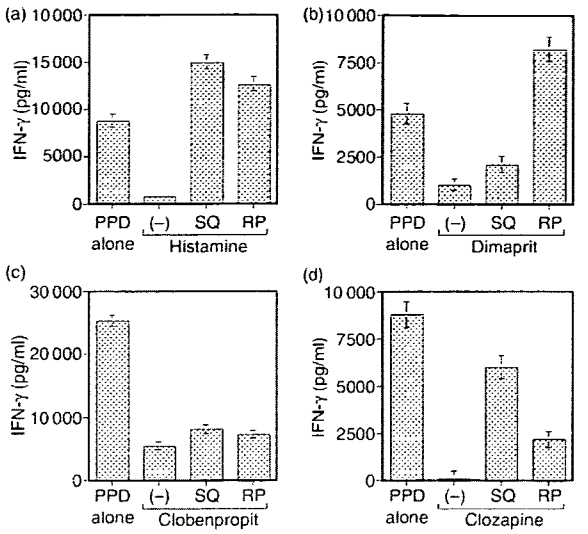

Figure 6. Roles of cAMP and protein kinase A (PKA) in the inhibition of purified protein derivative of *Mycobacterium tuberculosis* (PPD)-induced interferon-γ (IFN-γ) production by H4R-selective agonists. Peripheral blood mononuclear cells (PBMCs) were pretreated for 60 min with SQ22536 (SQ) or RP-8-Br-cAMPS (RP) and then incubated with 2 μg/ml of PPD and 100 μM histamine (a), dimaprit (b), clobenpropit (c), or clozapine (d). The results are expressed as the mean concentrations ± standard deviation (SD) from triplicate cultures. Data are representative of three separate experiments.

Pretreatment of PPD-specific TCLs alone with SQ22536, followed by coculture with intact APCs, partially suppressed inhibition of the PPD-specific IFN-γ production by dimaprit. Similar suppression was observed when APCs alone were pretreated with SQ22536, followed by the coculture with intact TCLs. However, pretreatment of both TCLs and APCs with SQ22536 markedly reversed the inhibitory effects of dimaprit on the PPD-specific response (Fig. 7).

The addition of 100 μM dimaprit, clobenpropit, or clozapine, but not of histamine, induced annexin-V expression on PBMCs (Fig. 8). $CD19^+$ cells were highly

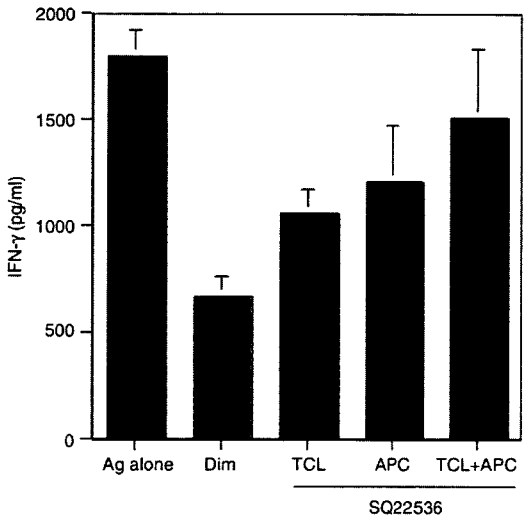

Figure 7. Reversal of H4R-selective agonist-induced inhibition of antigen (Ag)-specific T-cell responses with an adenylate cyclase inhibitor. Purified protein derivative of a *Mycobacterium tuberculosis* (PPD)-specific T-cell line (TCL) alone, antigen-presenting cells (APCs) alone, or both TCL and APC, were pretreated with SQ22536 at 37° for 1 hr. Following incubation, the cells were washed with culture medium three times, after which they were mixed and cultured with the PPD, in the presence of 100 μM dimaprit (Dim), for 65 hr. Data are representative of two separate experiments.

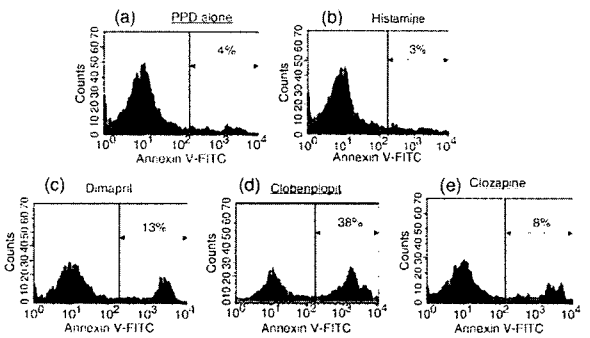

Figure 8. Expression of annexin-V by peripheral blood mononuclear cells (PBMCs) following treatment with H4R-selective agonists. PBMCs were incubated for 72 hr with purified protein derivative of *Mycobacterium tuberculosis* (PPD) (a) and histamine (b), dimaprit (c), clobenpropit (d), or clozapine (e), and the expression of annexin-V on $CD19^+$ cells was analysed by flow cytometry. Data are representative of six separate experiments.

susceptible to the induction of annexin-V expression following exposure to H4R-related agonists. H4R agonists also induced annexin-V expression in $CD4^+$ cells, but not in $CD8^+$ cells (data not shown).

cDNA miroarray analysis

We sought to compare the comprehensive expression of mRNA in PBMC following PPD stimulation in the presence or absence of clozapine. Among 16 600 genes tested, the amounts of mRNA were unchanged in 96·2% of the genes. However, the mRNA levels of 0·8% of the genes (such as melanocortin 1 receptor) were increased (> 200%) in the presence of clozapine. On the contrary, the mRNA levels of 3·0% of the genes, such as IFN-γ, were decreased (< 50%) (Table 1).

Effect of HR-selective agonists on Cry j1-induced IL-5 production

We examined the effect of HR-selective agonists on human Th2 responses. PBMCs from patients with Japanese cedar pollinosis produced a comparable amount of IL-5 in response to Cry j1. The addition of 100 μM 2-PEA, 4-MH or α-MH displayed no significant effect on Cry j1-induced IL-5 production. However, H4R agonists, including dimaprit, clobenpropit and clozapine, significantly inhibited Cry j1-induced IL-5 production (Fig. 9).

Expression of the four histamine receptors on Ag-specific TCLs

Finally, mRNA expression of the four histamine receptors was examined in five PPD- and five Cry j1-specific TCLs by reverse transcription–polymerase chain reaction (RT–PCR). H3R mRNA expression was completely undetectable in all TCLs. On the other hand, H1R, H2R and H4R mRNA were clearly detected in most TCLs (Fig. 10). Using real-time PCR analysis, relative expression levels of the four HRs were not observed to differ significantly among Cry j1- and PPD-specific TCLs (H1R, $P = 0{\cdot}117$; H2R, $P = 0{\cdot}245$; H4R, $P = 0{\cdot}344$; using the Mann–Whitney *U*-test). The expression levels of H4R in TCLs were lower than that of H1R; however, significantly increased expression of the H4R was observed as compared to H2R and H3R (Fig. 11).

Discussion

In the present study, we demonstrated that histamine inhibits PPD-induced IFN-γ production in PBMCs. Several studies have investigated the regulatory role of histamine on IFN-γ production by T cells.[7,8,14–16] Lagier *et al.* reported that histamine inhibits IFN-γ production by human Th1-like T-cell clones (TCCs) specific for *Dermatophagoides pteronyssinus*, whereas it did not have a significant inhibitory effect on T helper 0 (Th0)-like TCCs, and it had no effect on Th2-like TCCs stimulated with phorbol 12-myristate 13-acetate (PMA) and a calcium ionophore.[8] Krouwels *et al.* reported that histamine inhibited IFN-γ production in 21 out of 52 human TCCs (40%), whereas IFN-γ production was enhanced in eight of the TCCs (16%). Also, histamine did not affect IFN-γ production in 23 TCCs (44%) in response to plate-bound

Table 1. Ranked list of up-regulated and down-regulated transcripts in purified protein derivative of *Mycobacterium tuberculosis* (PPD)-stimulated peripheral blood mononuclear cells with clozapine

	Up-regulated transcripts				Down-regulated transcripts		
Rank	Gene name	GenBank acc. no.	Ratio[1]	Rank	Gene name	GenBank acc. no.	Ratio[1]
1	Melanocortin 1 receptor	NM_002386	8·50	1	Interferon-γ	NM_000619	0·02
2	LOC90271	XM_030445	5·59	2	Chemokine (C-C motif) ligand 5	NM_002981	0·02
3	ATP-binding cassette, subfamily G (WHITE) member 1, transcript variant 1	NM_004915	4·75	3	Matrix metalloproteinase 10	NM_002425	0·02
4	Actin-binding LIM protein 2	NM_032432	4·69	4	Chemokine (C-X-C motif) ligand 5	NM_002994	0·03
5	Liver-expressed antimicrobial peptide 2	NM_052971	4·32	5	KIAA1046 protein	NM_014928	0·03
6	Oviductal glycoprotein 1, 120 000 MW	NM_002557	4·30	6	Secreted phosphoprotein 1	NM_000582	0·03
7	Killer-specific secretory protein of 37 000 MW	NM_031950	3·96	7	Chemokine (C-X-C motif) ligand 1	NM_001511	0·03
8	LOC286006	XM_209854	3·83	8	Tumor necrosis factor (ligand) superfamily member 15	NM_005118	0·03
9	Myelin-basic protein	NM_002385	3·73	9	Similar to immune-responsive protein 1	XM_292184	0·04
10	Hypothetical protein LOC157562	XM_098779	3·71	10	Matrix metalloproteinase 7	NM_002423	0·04

[1]Ratio: with clozapine versus without clozapine.
GenBank acc. no., GenBank accession number; MW, molecular weight.

anti-CD3 mAb.[14] In contrast, pretreatment with histamine does enhance IFN-γ production in response to plate-bound anti-CD3 mAb in human Th1 cells.[7] Furthermore, Osna *et al.* showed that the effect of histamine on IFN-γ production was dependent on the stimulatory signals.[15]

We investigated the PPD-induced human T-cell responses to clarify whether histamine affects antigen-specific T-cell responses. Our results are consistent with previous reports. Osna *et al.* reported that histamine up-regulates IL-10 production in murine splenocytes and inhibits IFN-γ production.[16] In the current study, PBMCs did not produce IL-10 in response to PPD, and IL-10 production was not induced in the presence of histamine, suggesting that factors other than IL-10 may be involved in the inhibitory effect of histamine.

The H4R agonists dimaprit, clobenpropit and clozapine all eliminated PPD-induced proliferation and IFN-γ production in PBMCs. H4R is selectively expressed in cells of haematopoietic lineage, including mast cells, eosinophils and lymphocytes.[3,17] Physiological roles of H4R in mast cells, eosinophils, neutrophils and dendritic cells have been implied in recent years, but whether signals through H4R can affect T-cell functions has not been determined.[6,17–19] One report demonstrated that histamine induces IL-16 production by human $CD8^+$ T cells through H2R and H4R.[9] Our results, using HR-related agonists, suggest that signals through H4R may exert an inhibitory role on antigen-specific T-cell responses. However, thioperamide, an H3R and H4R antagonist, did not reverse the inhibition of PPD-induced IFN-γ production by either histamine or H4R agonists. Thioperamide, *d*-chlorpheniramine and famotidine, the HR antagonists used in the present study, were confirmed to be functional in previous studies.[20,21] This suggests that the inhibitory effect of histamine and H4R agonists is not mediated by H4R. In addition, a mixture of *d*-chlorpheniramine, famotidine and thioperamide did not reverse the inhibition by histamine, suggesting that the effect is independent of H1R, H2R and H3R/H4R.

2-PEA, an H1R-selective agonist, did not affect PPD-induced IFN-γ production. On the other hand, 4-MH, an H2R-selective agonist, partially inhibited its production. It is known that histamine regulates cytokine production, via H2R, on T cells.[8,14,15,22] In addition, histamine inhibits IL-12 production by monocytes via H2R.[23] Our finding that dimaprit, an H2R and H4R agonist, inhibited PPD-induced IFN-γ production, suggests that signals through H2R may be involved in the inhibition. However, the inhibitory effect of either histamine or dimaprit

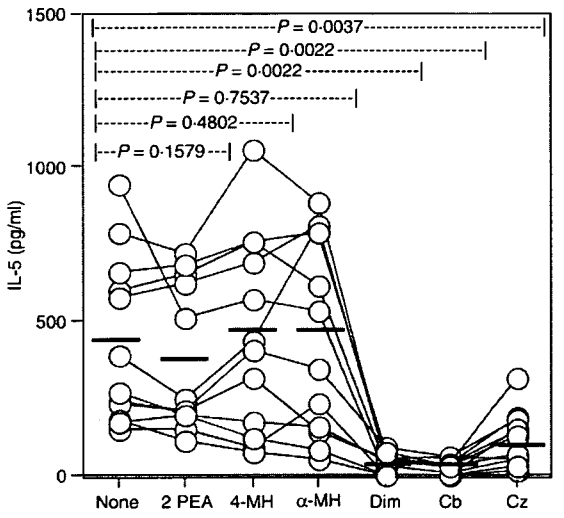

Figure 9. Histamine receptor (HR)-selective agonists-mediated inhibition of Cry j1-specific interleukin (IL)-5 production by peripheral blood mononuclear cells (PBMCs). PBMCs from 12 patients with Japanese cedar pollinosis were cultured with 10 μg/ml of Cry j1, in the presence or absence of 2-pyridylethylamine (2-PEA), 4-methylhistamine (4-MH), alpha-methylhistamine (α-MH), dimaprit (Dim), clobenpropit (Cb) or clozapine (Cz), at 100 μM, for 72 hr. Following incubation, supernatant was collected and the concentrations of IL-5 were determined in each sample using an enzyme-linked immunosorbent assay (ELISA). *P*-values were obtained using Wilcoxon's signed-rank test.

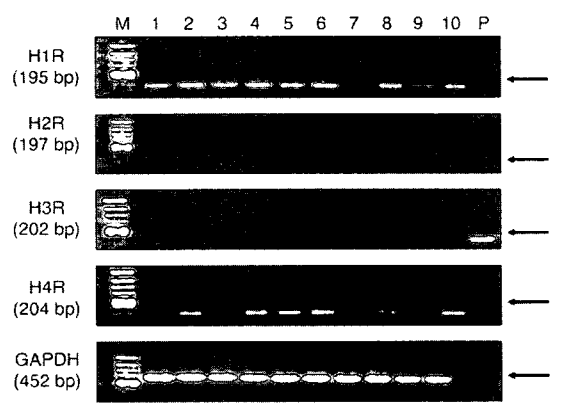

Figure 10. Expression of four histamine receptors (HRs) by human T-cell lines (TCLs). mRNA was extracted from five Cry j1-specific TCLs (lanes 1–5) and from five purified protein derivative of *Mycobacterium tuberculosis* (PPD)-specific TCLs (lanes 6–10), after which the levels of H1R, H2R, H3R, H4R and glyceraldehyde 3-phosphate dehydrogenase (GAPDH) were detected by reverse transcription–polymerase chain reaction (RT–PCR), as described in the Materials and methods. M, molecular marker; P, positive control (NEC14).

was not reversed by famotidine, suggesting that H2R signalling had a negligible role in the inhibition of PPD-induced IFN-γ production.

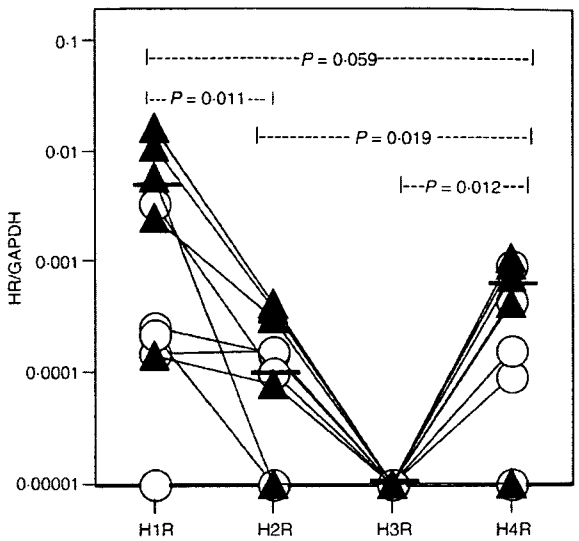

Figure 11. Comparison of the amounts of four histamine receptors (HRs) among T-cell lines (TCLs). The expression levels of four HRs were determined in five Cry j1-specific TCLs (closed triangle) and in five purified protein derivative of *Mycobacterium tuberculosis* (PPD)-specific TCLs (open circle) using real-time reverse transcription–polymerase chain reaction (RT–PCR). Each bar represents the median expression level of each messenger. *P*-values were obtained using Wilcoxon's signed-rank test.

The pretreatment of PBMCs with SQ22536, an adenylate cyclase inhibitor, and with RP-8-Br-cAMPS, a PKA type 1 inhibitor, reversed the inhibition of PPD-induced IFN-γ production by histamine and H4R agonists. Previous reports demonstrated that 5 mM SQ22536 and 5 mM RP-8-Br-cAMPS reversed, almost completely, the inhibitory effect of several compounds on human PBMC responses.[12] These results suggest that H4R agonists, except for clobenpropit, inhibit PPD-induced IFN-γ production by elevating intracellular cAMP levels and activating PKA. Moreover, results using PPD-specific TCLs and APCs suggest that H4R agonists may influence PPD-specific cellular responses at both the T-cell and APC level. It is known that H2R activation causes an elevation of the intracellular cAMP level.[24] In addition, PKA plays a pivotal role in histamine-mediated regulation of IFN-γ production, especially via the stimulation of T-cell receptors.[15] Although dimaprit can act as an H2R agonist, clozapine and clobenpropit cannot.[25] H4R is coupled to $G_{i/o}$, which leads to the inhibition of cAMP formation.[26] This further supports the possibility that the inhibitory effect of H4R agonists is not associated with typical H4R signaling. Rather, signals similar to those mediated by H2R may participate in the inhibition. However, we also observed that the inhibitory effect of either histamine or dimaprit was not reversed by famotidine, suggesting that H2R signaling had a negligible role in the inhibition of PPD-induced IFN-γ production. In addition, the varied effect of SQ22536 and RP-8-Br-cAMPS on IFN-γ

production induced by different agonists may suggest the presence of unidentified pleural receptors in the action of agonists.

$CD19^+$ and $CD4^+$ cells express annexin-V following exposure to H4R agonists, suggesting that these compounds induce apoptosis in these cells. On the other hand, cDNA microarray analysis revealed that the changes of mRNA levels were seen in 0·8% of the genes tested, such as melanocortin 1 receptor, following the stimulation with H4R agonist (Table 1), indicating that the inhibitory effects of H4R agonists were not non-specific or solely the result of an apoptotic effect. For example, melanocortin 1 receptor has signal transducer activity and it is involved in immunosuppression.[27] Thus, the suppressive role of H4R agonists may be associated with the activation of melanocortin 1 receptor. In addition, histamine did not induce the expression of annexin-V. These results suggest that the inhibitory effect of H4R agonists is not associated with the binding to classical HRs.

Concentrations of histamine and H4R agonists ranging from 10^{-5} to 10^{-4} M displayed a dose-dependent inhibition of PPD-induced IFN-γ production by PBMCs. Although it was difficult to define precisely the histamine concentration in the target organ, concentrations of histamine from 10^{-6} to 10^{-4} M have been reported to be comparable to those measured in tissues after mast cell degranulation.[28]

In conclusion, we examined the effect of histamine and H4R agonists on antigen-specific human T-cell responses. H4R signaling is important for functions of other immune cells, such as mast cell chemotaxis, eosinophil chemotaxis and suppression of IL-12 production by dendritic cells.[3,29] H4R agonists inhibit Ag-specific cytokine production; however, our investigations, using antagonists of H4R and inhibitors of adenylate cyclase or PKA, revealed that H4R plays a negligible role in the inhibition. These results indicate that there may be a previously unidentified HR or receptor subtype that can bind to dimaprit, clobenpropit and clozapine and that can mediate the inhibition of antigen-induced cellular responses via a cAMP/PKA-dependent, apoptotic pathway. More recently, Lim *et al.* have reclassified 4-MH as the most selective H4R agonist so far at the H4R.[30] This seems to be relevant for understanding the present results, suggesting a new orphan receptor. Furthermore, our observations may provide the basis for novel therapeutic approaches in the management of allergic and autoimmune diseases.

Acknowledgements

The authors would like to thank Yuko Okano for her editorial assistance. This work was supported, in part, by grants from Research on Allergic disease and Immunology of Ministry of Health, Labor and Welfare (no. 14210301 to MO).

References

1 Akdis CA, Simons FER. Histamine receptors are hot in immunopharmacology. *Eur J Pharmacol* 2006; **533**:69–76.
2 Oda T, Morikawa N, Saito Y, Masuho Y, Matsumoto S. Molecular cloning and characterization of a novel type of histamine receptor preferentially expressed in leukocytes. *J Biol Chem* 2000; **275**:36781–6.
3 de Esch IJP, Thurmond RL, Jongejan A, Leurs R. The histamine H4 receptor as a new therpeutic target for inflammation. *Trends Pharmacol Sci* 2005; **26**:462–9.
4 Ling P, Ngo K, Nguyen S, Thurmond RL, Edwards JP, Karlsson L, Fung-Leung W. Histamine H4 receptor mediates eosinophil chemotaxis with cell shape change and adhesion molecule upregulation. *Br J Pharmacol* 2004; **142**:161–71.
5 O'Reilly M, Alpert R, Jenkinson S *et al.* Identification of a histamine H4 receptor on human eosinophils – role in eosinophil chemotaxis. *J Recept Signal Transduct Res* 2002; **22**:431–48.
6 Gutzmer R, Diestel C, Mommert S, Kother B, Stark H, Wittmann M, Werfel T. Histamine H4 receptor stimulation suppresses IL-12p70 production and mediates chemotaxis in human monocyte-derived dendritic cells. *J Immunol* 2005; **174**:5224–32.
7 Jutel M, Watanabe T, Klunker S *et al.* Histamine regulated T-cell and antibody responses by differential expression of H1 and H2 receptors. *Nature* 2001; **413**:420–5.
8 Lagier B, Lebel B, Bousquet J, Pene J. Different modulation by histamine of IL-4 and interferon-gamma (IFN-γ) release according to phenotype of human Th0, Th1, Th2 clones. *Clin Exp Immunol* 1997; **108**:545–51.
9 Gantner F, Sakai K, Tusche MW, Cruikshank WW, Center DM, Bacom KB. Histamine H4 and H2 receptors control histamine-induced interleukin-16 release from human CD8+ T cells. *J Pharmacol Exp Ther* 2002; **303**:300–7.
10 Okano M, Sugata Y, Fujiwara T *et al.* E prostanoid 2 (EP2)/EP4-mediated suppression of antigen-specific human T cell responses by prostaglandin E2. *Immunology* 2006; **118**:343–52.
11 Okano M, Kino K, Takishita T, Hattori H, Ogawa T, Yoshino T, Yokoyama M, Nishizaki K. Roles of carbohydrates on Cry j 1, the major allergen of Japanese cedar pollen, in specific T-cell responses. *J Allergy Clin Immunol* 2001; **108**:101–8.
12 Aandahl EM, Moretto WJ, Haslett PA, Vang T, Bryn T, Tasken K, Nixon DF. Inhibition of antigen-specific T cell proliferation and cytokine production by protein kinase A Type I. *J Immunol* 2002; **169**:802–8.
13 Motoyama T, Watanabe H, Yamamoto T, Sekiguchi M. Human testicular germ cell tumors *in vitro* and in athymic nude mice. *Acta Pathol Jpn* 1987; **37**:431–48.
14 Krouwels FH, Hol BEA, Lutter R, Bast A, Jansen HM, Out TA. Histamine affects interleukin-4, and interferon-γ production by human T cell clones from the airways and blood. *Am J Respir Cell Mol Biol* 1998; **18**:721–30.
15 Osna N, Elliott K, Khan MM. The effects of histamine on interferon gamma production are dependent on the stimulatory signals. *Int Immunopharmacol* 2001; 1:135–45.
16 Osna N, Elliott K, Khan MM. Regulation of interleukin-10 secretion by histamine in TH2 cells and splenocytes. *Int Immunopharmacol* 2001; 1:85–96.
17 Liu C, Ma X, Jiang X, Wilson SJ *et al.* Cloning and pharmacological characterization of a fourth histamine receptor (H4) expressed in bone marrow. *Mol Pharamcol* 2001; **59**:420–6.

18 Buckland KF, Williams TJ, Conroy DM. Histamine induces cytoskeletal change in human eosinophils via the H4 receptor. *Br J Pharmacol* 2003; **140**:1117–27.

19 Takeshita K, Sakai K, Bacon KB, Gantner F. Critical role of histamine H4 receptor in leukotriene B4 production and mast cell-dependent neutrophil recruitment induced by zymosan *in vivo*. *J Pharmacol Exp Ther* 2003; **307**:1072–8.

20 Ito Y, Oishi R, Nishibori M, Saeki K. Characterization of histamine release from the rat hypothalamus as measured by *in vivo* microdialysis. *J Neurochem* 1991; **56**:769–74.

21 Yokoyama M, Yokoyama A, Mori S *et al.* Inducible histamine protects mice from *P. acnes*-primed and LPS-induced hepatitis through H2-receptor stimulation. *Gastroenterology* 2004; **127**:892–902.

22 Poluektova LY, Khan MM. Protein kinase A inhibitors reverse histamine-mediated regulation of IL-5 secretion. *Immunopharmacology* 1998; **39**:9–19.

23 Elenkov IJ, Webster E, Panicolaou DA, Fleisher TA, Chrousos GP, Wilder RL. Histamine potently suppresses human IL-12 and stimulates IL-10 production via H2 receptors. *J Immunol* 1998; **161**:2586–93.

24 Gantz I, Munzert G, Tashiro T, Schaffer M, Wang L, Delvalle J, Yamada T. Molecular cloning of human histamine H2 receptor. *Biochem Biophys Res Commun* 1991; **178**:1386–92.

25 Hough LB. Genomics meets histamine receptors: new subtypes, new receptors. *Mol Pharmacol* 2001; **59**:415–9.

26 Nakamura T, Itadani H, Hidaka Y, Ohta M, Tanaka K. Molecular cloning and characterization of a new human histamine receptors, HH4R. *Biochem Biophys Res Commun* 2000; **279**:615–20.

27 Cooper A, Robinson SJ, Rickard C, Jackson CL, Friedmann PS, Healy E. Alpha-melanocyte-stimulating hormone suppresses antigen-induced lymphocyte stimulation in humans independently of melanocortin 1 receptor gene status. *J Immunol* 2005; **175**:4806–13.

28 Jeannin P, Delneste Y, Gosset P, Molet S, Lassale P, Hamid Q, Tsicopoulos A, Tonnel AB. Histamine induces interleukin-8 secretion by endothelial cells. *Blood* 1994; **84**:2229–33.

29 Hofstra CL, Desai PJ, Thurmond RL, Fung-Leung WP. Histamine H4 receptor mediates chemotaxis and calcium mobilization of mast cells. *J Pharmacol Exp Ther* 2003; **305**: 1212–21.

30 Lim HD, van Rijin RM, Ling P, Bakker RA, Thurmond RL, Leurs R. Evaluation of histamine H1-, H2-, and H3-receptor ligands at the human histamine H4 receptor: identification of 4-methylhistamine as the first potent and selective H4 receptor agonist. *J Pharmacol Exp Ther* 2005; **314**:1310–21.

Biosci. Biotechnol. Biochem., **72** (2), 485–491, 2008

Glycoform Analysis of Japanese Cypress Pollen Allergen, Cha o 1: A Comparison of the Glycoforms of Cedar and Cypress Pollen Allergens

Yoshinobu KIMURA,[1,2,†] Misao KUROKI,[2] Megumi MAEDA,[1,*] Mitsuhiro OKANO,[3] Minehiko YOKOYAMA,[4] and Kosuke KINO[4]

[1]*Department of Biofunctional Chemistry, Graduate School of Natural Science and Technology, Okayama University, 1-1-1 Tsushima-Naka, Okayama 700-8530, Japan*
[2]*Department of Bioresources Chemistry, Faculty of Agriculture, Okayama University, 1-1-1 Tsushima-Naka, Okayama 700-8530, Japan*
[3]*Department of Otolaryngology-Head and Neck Surgery, Okayama University, Graduate School of Medicine and Dentistry, Okayama 700-8558, Japan*
[4]*Meiji Co., Odawara 250-0862, Japan*

Received September 5, 2007; Accepted October 18, 2007; Online Publication, February 7, 2008
[doi:10.1271/bbb.70572]

A Japanese cypress (*Chamaecyparis obtusa*) pollen allergen, Cha o 1, is one of the major allergens that cause allergic pollinosis in Japan. Although it has been found that Cha o 1 is glycosylated and that the amino acid sequence is highly homologous with that of Japanese cedar pollen allergen (Cry j 1), the structure of *N*-glycans linked to Cha o 1 remains to be determined. In this study, therefore, we analyzed the structures of the *N*-glycans of Cha o1. The *N*-glycans were liberated by hydrazinolysis from purified Cha o 1, and the resulting sugar chains were *N*-acetylated and pyridylaminated. The structures of pyridylaminated *N*-glycans were analyzed by a combination of exoglycosidase digestion, two dimensional (2D-) sugar chain mapping, and electrospray ionization mass spectrometry analysis. Structural analysis indicated that the major *N*-glycan structure of Cha o1 is GlcNAc2Man3Xyl1-Fuc1GlcNAc2 (89%), and that high-mannose type structures (Man9GlcNAc2, Man7GlcNAc2) occur as minor components (11%).

Key words: *N*-glycan structure; antigenic oligosaccharide; Japanese cypress pollen allergen; Cha o 1; *Chamaecyparis obtusa*

In previous studies,[1,2] we determined the chemical structures of *N*-glycans linked to two cedar pollen allergens, Cry j 1 (Japanese cedar pollen allergen) and Jun a 1 (mountain cedar pollen allergen), and revealed that biantennary plant complex type *N*-glycans harboring Lewis a epitope occur in their *N*-glycan moieties. This finding suggests that the Lewis a epitope may play a critical role in pollinosis, but the occurrence of this epitope in plant glycoallergens has been reported from only three pollen allergens, Cup a 1 (pollen allergen from Arizona cypress),[3] Cry j 1, and Jun a 1. Japanese cypress pollen is another major allergic pollen in Japan, and Cha o 1 is a major allergen contained in the cypress pollens. Although it is known that Cha o 1 is *N*-glycosylated,[4] the detailed chemical structures of the *N*-glycan moiety remain to be determined. Hence, in this study, we analyzed the structures of *N*-glycans linked to the Japanese cypress pollen allergen Cha o 1 to determine whether plant specific antigenic oligosaccharide or Lewis a epitope occurs in the allergen. First, we purified Cha o 1 from an extract of the cypress pollens by a combination of ion-exchange chromatography and gel-filtration, using an antiserum against Cha o 1 to monitor the elution position of the allergen. We found that Cha o 1 occured in two forms, with the same N-terminal amino acid sequence but different molecular weights, suggesting that the numbers of the *N*-glycosylation sites might be different from each other. Furthermore, structural analysis of *N*-glycans revealed

† To whom correspondence should be addressed. Fax: +81-86-251-8388; E-mail: yosh8mar@cc.okayama-u.ac.jp
* Present address: *Department of Hygiene, Kawasaki Medical School, 577 Matsushima, Kurashiki 701-0192, Japan*

Abbreviations: PA-, pyridylamino; RP-HPLC, reverse-phase HPLC; SF-HPLC, size-fractionation HPLC; ESI-MS, electrospray ionization mass spectrometry; CBB, Coomassie Brilliant Blue; Hex, hexose; HexNAc, *N*-acetylhexosamine; Deoxyhex, deoxyhexose; Pen, pentose; M3FX, Manα1-6(Manα1-3)(Xylβ1-2)Manβ1-4GlcNAcβ1-4(Fucα1-3)GlcNAc-PA; MFX, Xylβ1-2Manβ1-4GlcNAcβ1-4(Fucα1-3)GlcNAc-PA; GN2M3FX, GlcNAcβ1-2Manα1-6(GlcNAcβ1-2Manα1-3)(Xylβ1-2)Manβ1-4GlcNAcβ1-4(Fucα1-3)GlcNAc-PA; M9A, Manα1-2Manα1-6(Manα1-2Manα1-3)-Manα1-6(Manα1-2Manα1-2Manα1-3)Manβ1-4GlcNAcβ1-4GlcNAc-PA; M7A, Manα1-2Manα1-6(Manα1-3)Manα1-6(Manα1-2Manα1-3)Manβ1-4GlcNAcβ1-4GlcNAc-PA

that Cha o 1 bears both a biantennary complex type and a high-mannose type oligosaccharide. The predominant occurrence of the antigenic plant complex type structure, GlcNAc2Man3Xyl1Fuc1GlcNAc2 (GN2M3FX), is a characteristic common to allergenic pollen glycoproteins.[1-3] But the Lewis a unit was not found in the *N*-glycans of Cha o 1, in contrast with Cup a 1, Cry j 1, and Jun a 1, indicating that the Lewis a epitope is not involved in the symptoms of pollinosis.

Materials and Methods

Materials. An Asahipak NH2P-50 4E column (0.46 × 25 cm) was purchased from Showa Denko (Tokyo, Japan), and a Cosmosil 5C18-AR column (0.6 × 25 cm) from Nacalai Tesque (Kyoto, Japan). GN2M3FX were prepared from glycoproteins from rice culture cells.[5] M7A and M9A were prepared from royal jelly glycoproteins.[6] Antiserum against Cha o 1 was a generous gift of Meiji Co. Antiserum against β1-2 xylose-containing *N*-glycans was a generous gift of Dr. Arnd Strum (Friedrich-Miescher Institute, Basel, Switzerland).[7]

Purification of Cha o 1. Purification of Cha o 1 was basically done as described in a previous paper.[4] During the purification steps, the elution of Cha o 1 was monitored by immunoblotting assay using antiserum against Cha o 1. Japanese cypress pollen (100 g) was defatted in acetone (500 ml), and the resulting defatted pollen was suspended in 125 mM $(NH_4)_2CO_3$ and sonicated in an ice bath for 5 min. After incubation for 16 h at 4 °C, the extract was centrifuged at 8,000 rpm for 20 min, and the resulting supernatant was 80% saturated with ammonium sulfate. The protein precipitate was dissolved in a small amount of 10 mM Tris–HCl buffer, pH 7.8, and dialyzed against the same buffer (5-liter) for 2 d. After centrifugation, the resulting supernatant (total $OD_{280\,nm}$, $A_{280\,nm}$ × sample volume = 717.60) was applied to a DEAE cellulose column (4 × 40 cm) equilibrated with 10 mM Tris–HCl buffer, pH 7.8. The run-through fraction was pooled and dialyzed against 10-liter (5-liter × 2 times) of 10 mM Na-acetate buffer, pH 5.0, containing 0.1 M NaCl for 2 d. The dialyzate was applied to a SP-Toyopearl (3 × 22 cm) column equilibrated with the same buffer. After the column was washed with the same buffer (about 600 ml), bound proteins were eluted by 10 mM Na-acetate buffer, pH 5.0, containing 0.5 M NaCl. The bound fraction (the Cha o 1 fraction) was dialyzed against 10-liter (5-liter × 2 times) of 10 mM Na-acetate buffer, pH 5.0, containing 0.1 M NaCl for 2 d, and the resulting dialysate (total $OD_{280\,nm}$ = 29.68) was applied to the SP-Toyopearl (3 × 22 cm) column equilibrated with the same buffer. In a second cation-exchange chromatography, the bound proteins were eluted by a linear gradient of NaCl from 0.1 M to 0.5 M in 10 mM Na-acetate buffer, pH 5.0. The Cha o 1 fraction, indicated by a horizontal bar in Fig. 1-A, was pooled and concentrated to about 7 ml by Amicon Centriprep-30. The total $OD_{280\,nm}$ of the concentrated sample was 5.26. Cha o1 was further purified by gel-filtration with a Superdex 200 column (GE-Healthcare, 1.6 × 120 cm) in 25 mM Tris–HCl buffer, pH 7.8, containing 0.1 M NaCl. As shown in Fig. 1-B, Cha o 1 was separated from some other contaminative proteins, but two protein bands (around 47 kDa) were detected on the SDS-gel by CBB staining (Fig. 2-I) and on the PVDF membrane by immunoblotting using the antiserum against Cha o 1 (Fig. 2-II), suggesting that Cha o 1 occurs in several isoforms, as reported by Suzuki *et al.*[4] Furthermore, as shown in Fig. 2-III, the purified Cha o 1 was recognized by the

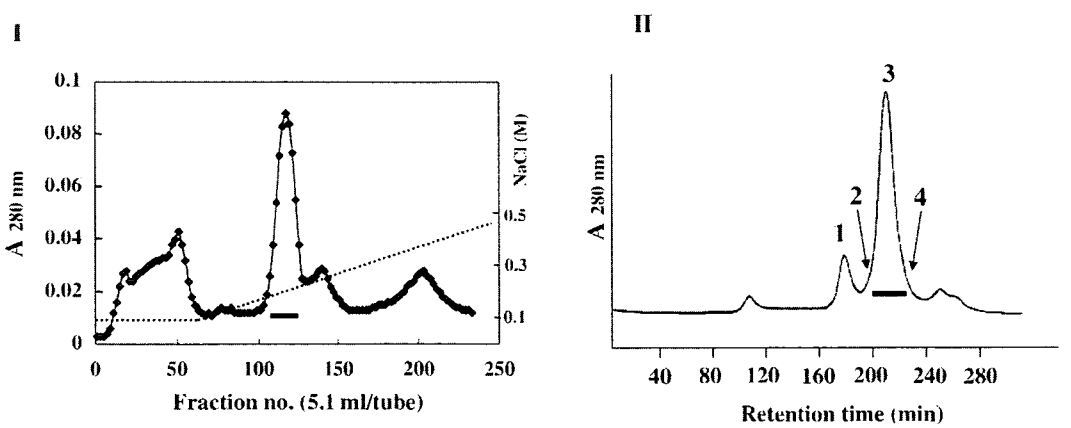

Fig. 1. Purification of Cha o 1.

I, SP-Toyopearl chromatography of partially purified Cha o1. Partially purified Cha o 1 was loaded on a SP-Toyopearl column in 10 mM Na-acetate buffer, pH 5.0. The allergen was eluted by a linear gradient of NaCl from 0.1 M to 0.5 M in 10 mM Na-acetate buffer, pH 5.0. The Cha o 1-containing fraction, detected by immunoblotting, was pooled, as indicated by a horizontal bar. II, Gel-filtration of the Cha o 1 fraction obtained in I. The concentrated Cha o 1 fraction obtained by SP-Toyopearl chromatography was loaded on a Superdex 200 column (1.6 × 120 cm). The column was developed with 25 mM Tris–HCl buffer, pH 7.8, containing 0.1 M NaCl at a flow rate of 0.8 ml/min.

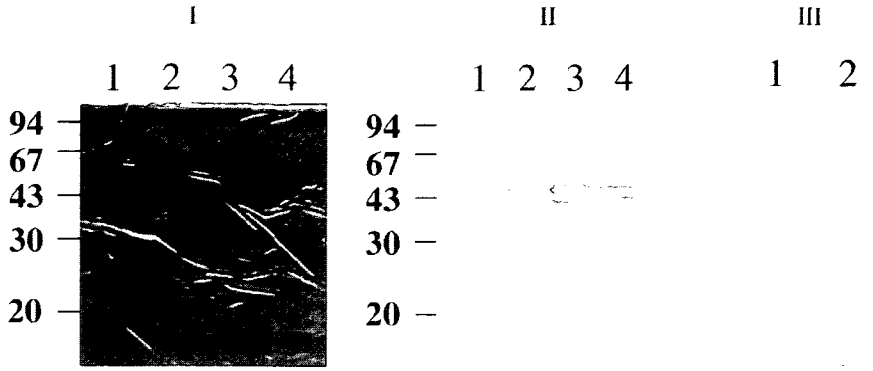

Fig. 2. SDS–PAGE and Immunoblotting.
I, CBB staining of 20% polyacrylaminde gel. Lane 1, peak 1 in Fig. 1-II; lane 2, position 2 in Fig. 1-II; lane 3, peak 3 in Fig. 1-II; lane 4, position 4 in Fig. 1-II. II, Immunoblotting using anti-Cha o 1 antibody. Lane 1, peak 1 in Fig. 1-II; lane 2, position 2 in Fig. 1-II; lane 3, peak 3 in Fig. 1-II; lane 4, position 4 in Fig. 1-II. III, Immunoblotting using anti-β1-2xylose antibody. Lane 1, peak 1 in Fig. 1-II; lane 2, peak 3 in Fig. 1-II. Each immunoblot was done as described in previous papers.[4,8]

anti-β1-2 xylose antibody,[7,8] indicating that Cha o 1 bears plant-complex type *N*-glycans. After two protein bands were cut on PVDF membrane separately, each N-terminal amino acid sequence was analyzed, and it was found that the two proteins had the same N-terminal sequence (D-N-P-I-D-), indicating that they were Cha o 1. Based on these results, we used the Cha o 1 fraction, indicated by a horizontal bar in Fig. 1-II, in glycoform analysis without further purification.

Preparation of pyridylaminated N-glycans from Cha o 1. *N*-Glycans were released by hydrazinolysis (100 °C, 12 h, in 200 µl of anhydrous hydrazine) from the lyophilized Cha o 1 (2.6 mg). After *N*-acetylation of the hydrazinolysate with saturated ammonium bicarbonate (400 µl) and acetic anhydride (20 µl), the acetylated hydrazinolysate was desalted using Dowex 50 × 2 resins. Pyridylamination of the sugar chains was done by the method of Natsuka and Hase.[9] Separation of PA-sugar chains was done by HPLC on a Jasco 880-PU HPLC apparatus with a Jasco 821-FP Intelligent Spectrofluorometer, using the Shodex Asahipak NH2P-50 column (0.46 × 25 cm) and the Cosmosil 5C18-AR column (0.6 × 25 cm). On the Cosmosil 5C18-AR column, the PA-sugar chains were eluted by increasing the acetonitrile concentration in 0.05% TFA linearly from 0 to 10% at a flow rate 1.2 ml/min. In the case of size-fractionation HPLC using the Asahipak NH2P-50 column, the PA-sugar chains were eluted by increasing the water content in the water-acetonitrile mixture from 36% to 62% linearly for 60 min at a flow rate of 0.7 ml/min.

Electrospray ionization (ESI) mass spectrometry. ESI-MS analysis of PA-sugar chains was done as described in our previous reports,[5,6] using a Perkin Elmer Sciex API-III triple-quadrupole mass spectrometer with an atmospheric-pressure ionization ion source.

Glycosidase digestion of PA-sugar chains. Digestion with jack bean α-mannosidase, diplococcal β-*N*-acetylglucosaminidase, and *Aspergillus* α-1,2-mannosidase was done using about 200 pmol of the PA-sugar chains under the conditions described in our previous reports.[5,10] The resulting glycosidase-digests were analyzed by SF-HPLC using the Asahipak NH2P-50 column (0.46 × 25 cm).

Results and Discussion

Purification of PA-sugar chains

First, the PA-sugar chains from Cha o 1 were partially purified by RP-HPLC, as shown in Fig. 3. Three peaks

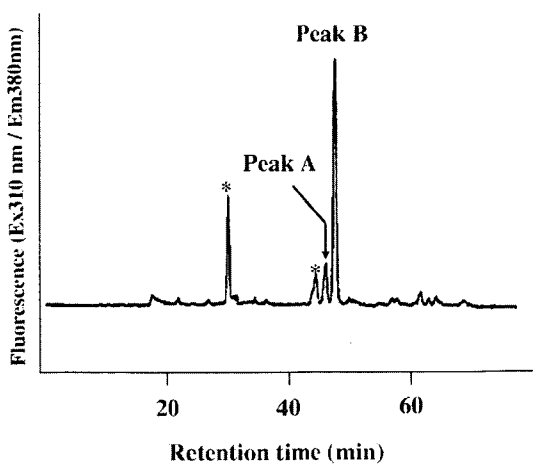

Fig. 3. RP-HPLC Profiles of PA-Sugar Chains from Cha o 1.
Peak A and peak B were confirmed to be relevant N-glycans by ESI-MS, and were used for structural analysis. PA-derivatives were loaded on the Cosmosil 5C 18-AR column (6.0 × 250 mm) equilibrated with 0.05% TFA. The PA-sugar chains were eluted by an increase in acetonitrile concentration. Star mark (*) shows contaminative peaks.

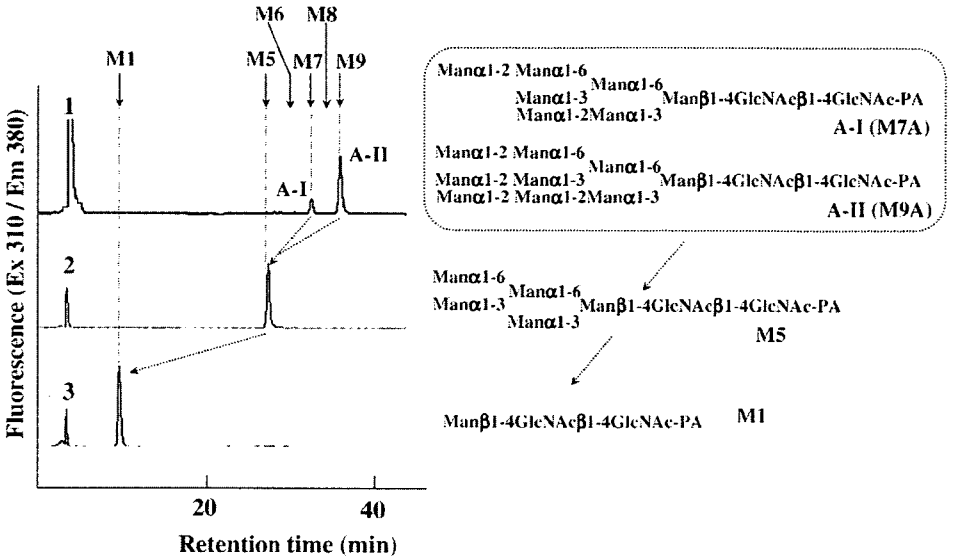

Fig. 4. SF-HPLC of Exoglycosidase Digests of Peak A.

1, PA-sugar chains in peak A in Fig. 3; 2, the *Aspergillus* α-1,2-mannosidase digest of 1; 3, the jack bean α-mannosidase digest of 2. Arrows (M1, M5, M6, M7, M8, and M9) indicate the elution positions of authentic PA-sugar chains: Man1GlcNAc2-PA, Man5GlcNAc2-PA, Man6GlcNAc2-PA, Man7GlcNAc2-PA, Man8GlcNAc2-PA, and Man9GlcNAc2-PA.

were observed in the region where *N*-glycans are expected to be eluted (40–70 min), but it was determined by exoglycosidase digestion that peaks A and B were relevant pyridylaminated *N*-glycans. A small peak eluted just before peak A was not digested by some exoglycosidases, suggesting that this peak might not be *N*-glycan, although MS/MS analysis of it to confirm the presence of GlcNAc-PA (*m/z* 300) could not be done due to the small amount of the sample.

Structures of PA-sugar chains peak A

When peak A in Fig. 3 was analyzed by SF-HPLC, two PA-sugar chains were detected, as shown in Fig. 4-1. The elution positions of these two PA-sugar chains corresponded to those of authentic PA-sugar chains: A-I to Man7GlcNAc2 and A-II to Man9-GlcNAc2-PA. Furthermore, the elution positions of A-I and A-II on RP-HPLC corresponded to those of M7A and M9A respectively. When these PA-sugar chains were treated with *Aspergillus* α-1,2-mannosidase, a new product was eluted at the elution position of M5A (Man5GlcNAc2-PA), suggesting that A-I and A-II contained two and four α1-2 mannose residues respectively (Fig. 4-2). The product was further converted to M1 (Man1GlcNAc2-PA) by jack bean α-mannosidase, as shown in Fig. 4-3.

From these results, the structures of A-I and A-II were proposed to be M7A and M9A, respectively, as shown in Fig. 4.

Structural analysis of N-glycans in peak B

As shown in Fig. 5-I, only one PA-sugar chain was detected in peak B in Fig. 3. The elution position corresponded to that of GN2M3FX. The elution position of this PA-sugar chain on RP-HPLC also corresponded to that of GN2M3FX (data not shown), suggesting that the structure of this *N*-glycan is the biantennary plant complex type structure, GlcNAc2Man3Xyl1Fuc1GlcNAc2. ESI-MS analysis of peak B showed a single signal at *m/z* 1674.5 $[(M + H)^+]$ (Fig. 5-II), suggesting that this PA-sugar chain consisted of (HexNAc)3(Hex)3(Deoxyhex)1(Pen)1(HexNAc-PA) or GlcNAc2-Man3Xyl1Fuc1GlcNAc2-PA. The deduced structure was further confirmed by exoglycosidase digestion. This PA-sugar chain was converted to M3FX with diplococcal β-*N*-acetylglucosaminidase, suggesting that two GlcNAc residues were bound by a β1-2 linkage (Fig. 5-I-2). The product was further converted to MFX by jack bean α-mannosidase digestion (Fig. 5-I-3). The data of 2-D sugar chain mapping, exoglycosidase digestion, and ESI-MS analysis suggested that the structure of peak B was GN2M3FX, as shown in Fig. 5.

Comparison of structural feature of N-glycans linked to cedar pollen allergen (Jun a 1 and Cry j 1) and cypress pollen allergen (Cha o 1)

As shown in Table 1, we have found that the cedar pollen allergens (Jun a 1 and Cry j 1) carry plant-complex type *N*-glycans containing the Lewis a antigen (Galβ1-3(Fucα1-4)GlcNAcβ1-) unit.[1,2] In addition to these two cedar pollen allergens, it has been reported that Arizona cypress pollen allergen, Cup a 1, also bears the Lewis a unit in the *N*-glycan moiety.[3] Although the physiological function of the Lewis a unit in plant *N*-glycans is still obscure, there is a possibility that the antigenic unit is involved in the symptoms of pollinosis.

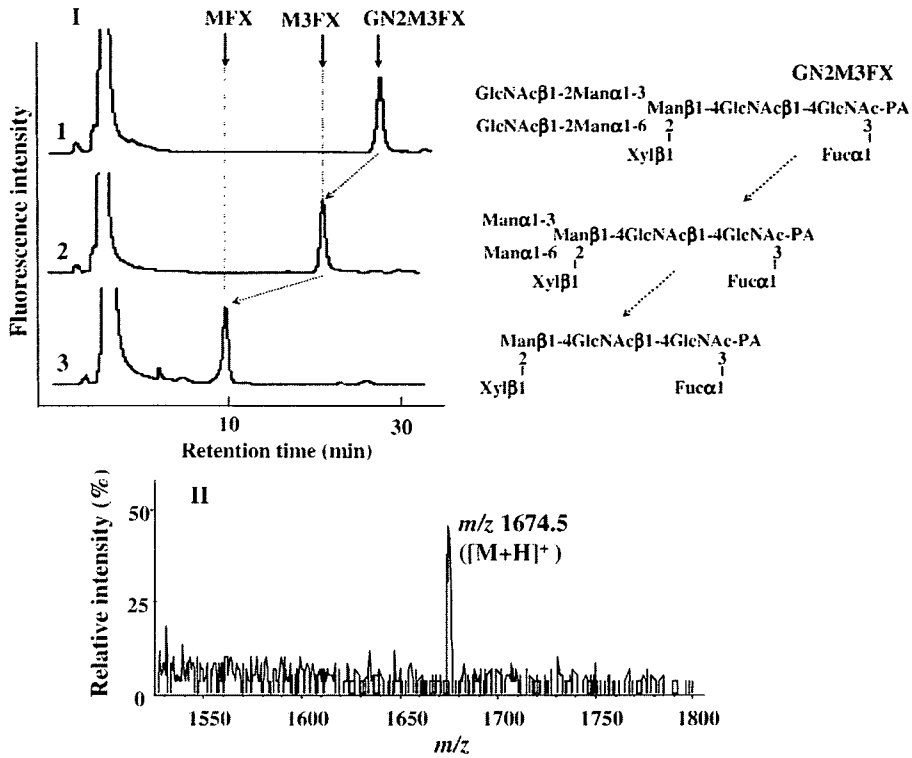

Fig. 5. SF-HPLC of Exoglycosidase Digests of Peak B and ESI-MS Spectrum.

I, SF-HPLC of exoglycosidase digests of peak B. 1, PA-Sugar chain in peak B in Fig. 3; 2, the diplococcal β-GlcNAc-ase digest of I; 3, the jack bean α-mannosidase digest of 2. II, ESI-MS spectrum of Peak B. The PA-sugar chain was observed as a single charged ion, $[M + H]^+$.

Table 1. Comparison of *N*-Glycan Structures of Two Cedar Pollen Allergens (Jun a 1, Cry j 1) and Cha o 1

Structures of *N*-Glycans	Jun a 1-A[a]	Jun a 1-B[a]	Cry j 1[b]	Cha o 1
GlcNAcβ1-2 {Manα1-6, Manα1-3} Manβ1-4GlcNAcβ1-4GlcNAc; Xylβ1; Fucα1	ND	3%	ND	ND
GlcNAcβ1-2Manα1-6, GlcNAcβ1-2Manα1-3 Manβ1-4GlcNAcβ1-4GlcNAc; Xylβ1; Fucα1	75%	76%	47%	89%
Fucα1-4Galβ1-3GlcNAcβ1-2Manα1-6, Manα1-3 Manβ1-4GlcNAcβ1-4GlcNAc; Xylβ1; Fucα1	23%	21%	38%	ND
Fucα1-4Galβ1-3GlcNAcβ1-2Manα1-6, Galβ1-3GlcNAcβ1-2Manα1-3 Manβ1-4GlcNAcβ1-4GlcNAc; Xylβ1; Fucα1	2%	ND	15%	ND
Manα1-2Manα1-6, Manα1-2Manα1-3 Manα1-6, Manα1-2Manα1-2Manα1-3 Manβ1-4GlcNAcβ1-4GlcNAc	ND	ND	ND	9%
Manα1-2Manα1-6, Manα1-3 Manα1-6, Manα1-2Manα1-3 Manβ1-4GlcNAcβ1-4GlcNAc	ND	ND	ND	2%

a, reference 1; b, reference 2

Hence, in this study, we analyzed the glycoform of *N*-glycans of Japanese cypress pollen allergen, Cha o 1, one of the major pollen glycoallergens in Japan. Molecular cloning of Cha o 1 revealed that this Japanese cypress pollen allergen is highly homologous with the two cedar pollen allergens (Cry j 1 and Jun a 1), and that there are six Asn-X-Thr/Ser sequences.[4] Although two (Asn(259)-Pro-Thr(261) and Asn(272)-Asp-Thr(274)) of them might not be glycosylated, it is not known whether the remaining four *N*-glycosylation sites are actually glycosylated. As described in a previous report,[4] Cha o 1 was purified in two isoforms with the same *N*-terminal amino acid sequence (D-N-D-I-P) but different molecular weights (Fig. 2-I), and these two isoforms were recognized by the antiserum against plant complex type *N*-glycans (Fig. 2-III). The difference in molecular weight of the two Cha o 1 molecules might reflect the difference in the numbers of actually glycosylated sites in the four *N*-glycosylation consensus sequences.

Structural analysis of *N*-glycans revealed that the complex type *N*-glycan harboring the Lewis a epitope did not occur in Cha o 1 and that major structure was the biantenary plant complex type structure: GlcNAc-β1-2Manα1-6(GlcNAcβ1-2Manα1-3)(Xylβ1-2)Manβ1-4GlcNAcβ1-4 (Fucα1-3)GlcNAc (GN2M3FX) (Fig. 5 and Table 1). This result suggest that the Lewis a epitope in the *N*-glycan moiety is not involved in the symptoms of pollinosis. It is noteworthy, however, that a high content of the GM2M3FX structure is a common feature of the *N*-glycans of allergenic pollen glycoproteins (Jun a 1, Cry j 1, Cup a 1, olive pollen allergen Ole e1, *Ginkgo biloba* pollen glycoprotein, and palm pollen glycoprotein).[1–3,11–13] Comparing the cedar pollen allergens (Jun a 1 and Cry j 1) and Arizona cypress pollen allergens (Cup a 1), the occurrence of high-mannose type *N*-glycans appears to be specific to Japanese cypress pollen allergen (Cha o 1), although the content is very low. Among plant glycoallergens, it has been reported that a peanut allergen, Ara h 1, carries the high-mannose type *N*-glycans (Man6-5GlcNAc2) in addition to xylosylated *N*-glycans.[11] And recently it has been proposed that the *N*-glycan of Ara h 1 is a ligand of dendritic cell-specific ICAM-grabbing nonintegrin (DC-SIGN) and that it acts as a Th2 ajuvant.[14] Since DC-SIGN is a C-type lectin specific to mannose residues in glycans, it is possible to assume that the *N*-glycans linked to Cha o 1 are ligands of DC-SIGN, and that Cha o 1 can prime Th2-skewed T-cell responses. Detail analysis of the immunological activity of the *N*-glycans of Cha o1 to dendritic cells is necessary to determine the involvement of plant *N*-glycans in the symptoms of pollinosis.

Acknowledgments

This work was supported in part by grants from the Ministry of Education, Culture, Sports, Science, and Technology of Japan (Basic Research (C), no. 17580300) and the Okayama University COE program, Establishment of Plant Health Science. The authors are grateful to the ESI-MS Laboratory of Okayama University.

References

1) Kimura, Y., Kamamoto, M., Maeda, M., Okano, M., Yokoyama, M., and Kino, K., Occurrence of Lewis a epitope in N-glycans of a glycoallergen, *Jun a 1*, from mountain cedar pollen. *Biosci. Biotechnol. Biochem.*, **69**, 137–144 (2005).
2) Maeda, M., Kamamoto, M., Yamamoto, S., Kimura, M., Okano, M., and Kimura, Y., Glycoform analysis of Japanese cedar pollen allergen, Cry j1. *Biosci. Biotechnol. Biochem.*, **69**, 1700–1705 (2005).
3) Alisi, C., Afferni, C., Iacovacci, P., Barletta, B., Tinghino, R., Butteroni, C., Puggioni, E. M. R., Wilson, I. B. H., Federico, R., Schinina, M. E., Ariano, R., Di Felice, G., and Pini, C., Rapid isolation, charcterization, and glycan analysis of Cup a 1, the major allergen of Arizona cypress (*Cupressus arizonica*) pollen. *Allergy*, **56**, 978–984 (2001).
4) Suzuki, M., Komiyama, N., Itoh, M., Itoh, H., Sone, T., Kino, K., Takagi, I., and Ohta, N., Purification, characterization and molecular cloning of Cha o 1, major allergen of *Chamaecyparis obtuse* (Japanese cypress) pollen. *Mol. Immunol.*, **33**, 451–460 (1996).
5) Maeda, M., and Kimura, Y., Glycoform analysis of *N*-glycans linked to glycoproteins expressed in rice culture cells: predominant occurrence of complex type *N*-glycans. *Biosci. Biotechnol. Biochem.*, **70**, 1356–1363 (2006).
6) Kimura, Y., Miyagi, C., Kimura, M., Nitoda, T., Kawai, N., and Sugimoto, H., Structural features of *N*-glycans linked to royal jelly glycoproteins. *Biosci. Biotechnol. Biochem.*, **64**, 2109–2120 (2000).
7) Kimura, Y., Hess, D., and Strum, A., The *N*-glycans of jack bean α-mannosidase: structure, topology, and function. *Eur. J. Biochem.*, **264**, 168–175 (1999).
8) Kimura, Y., Harada, T., Matsuo, S., and Yonekura, M., Purification and some chemical properties of 30 kDa *Ginkgo biloba* glycoprotein, which reacts with antiserum against β1→2 xylose-containing N-glycans. *Biosci. Biotechnol. Biochem.*, **63**, 163–167 (1999).
9) Natsuka, S., and Hase, S., Analysis of *N*- and *O*-glycans by pyridylamination. *Methods Mol. Biol.*, **76**, 101–113 (1998).
10) Kato, T., Kitamura, K., Maeda, M., Kimura, Y., Katayama, T., Ashida, H., and Yamamoto, K., Free oligosaccharides in the cytosol of *Caenorhabditis elegance* are generated through endoplasmic reticulum-Golgi trafficking. *J. Biol. Chem.*, **282**, 22080–22088 (2007).
11) Kolarich, D., and Altmann, F., N-Glycan analysis by matrix-assisted laser desorption/ionization mass spectrometry of electrophoretically separated nonmammalian proteins: application to peanut allergen Ara h 1 and olive pollen allergen Ole e 1. *Anal. Biochem.*, **285**, 64–75 (2000).
12) Kimura, Y., Suzuki, M., and Kimura, M., *N*-Linked oligosaccharides of glycoproteins from allergenic

Ginkgo biloba pollen. *Biosci. Biotechnol. Biochem.*, **65**, 2001–2006 (2001).

13) Kimura, Y., Yoshiie, T., Woo, K. K., Maeda, M., Kimura, M., and Tan, S. H., Structural features of *N*-glycans linked to glycoproteins from oil palm pollen, an allergenic pollen. *Biosci. Biotechnol. Biochem.*, **67**, 2232–2239 (2003).

14) Shreffler, W. G., Castro, R. R., Kucuk, Z. Y., Charlos-Powers, Z., Grishina, G., Yoo, S., Burks, A. W., and Sampson, H. A., The major glycoprotein allergen from *Arachis hypogaea*, Ara h 1, is a ligand of dendritic cell-specific ICAM-grabbing nonintegrin and acts as a Th2 adjuvant *in vitro*. *J. Immunol.*, **177**, 3677–3685 (2006).

Available online at www.sciencedirect.com
ScienceDirect
Molecular Immunology 44 (2007) 2249–2256
Molecular Immunology
www.elsevier.com/locate/molimm

Chromatin remodeling at the Th2 cytokine gene loci in human type 2 helper T cells

Takaaki Kaneko[a,b], Hiroyuki Hosokawa[a], Masakatsu Yamashita[a], Chrong-Reen Wang[c], Akihiro Hasegawa[a], Motoko Y. Kimura[a], Masayuki Kitajiama[a], Fumio Kimura[b], Masaru Miyazaki[b], Toshinori Nakayama[a,]

[a] *Department of Immunology, Graduate School of Medicine, Chiba University, 1-8-1 Inohana, Chuo-ku, Chiba 260-8670, Japan*
[b] *Department of General Surgery, Graduate School of Medicine, Chiba University, 1-8-1 Inohana, Chuo-ku, Chiba 260-8670, Japan*
[c] *Section of Allergy, Immunology and Rheumatology, Department of Internal Medicine, Medical College, National Cheng Kung University, Tainan, Taiwan*

Received 25 August 2006; received in revised form 1 November 2006; accepted 6 November 2006
Available online 12 December 2006

Abstract

The differentiation of mouse naïve CD4 T cells into type 2 helper (Th2) cells is accompanied by chromatin remodeling at the nucleosomes associated with the IL-4, IL-13 and IL-5 genes. However, little is known about how chromatin remodeling of these Th2 cytokine gene loci occurs in human Th2 cells. We herein established an *in vitro* culture system in which both Th1 and Th2 cells are efficiently differentiated from human peripheral blood naïve CD4 T cells. This system allowed us to investigate the chromatin status at the Th2 cytokine gene loci and the IFNγ locus in human Th2 and Th1 cells, respectively. In typical individuals, the chromatin remodeling indicated by the induction of hyper-acetylation of histone H3 lysine 9 and hyper-methylation of histone H3 lysine 4 was induced at the whole Th2 cytokine gene loci in developing Th2 cells. We more precisely assessed the methylation status of histone H3 lysine 4 at the Th2 cytokine gene loci (IL-5 exon 3, IL-5 promoter, IL-5/RAD50 intergenic region, RAD50 promoter, CGRE, CNS1, IL-13 promoter, IL-4 promoter, and V_A enhancer regions) and the IFNγ locus in developing Th1 and Th2 cells prepared from 20 healthy volunteers. Th2-cell specific chromatin remodeling was induced at most of the Th2 cytokine gene loci. In parallel with the induction of chromatin remodeling, GATA3 mRNA was preferentially expressed in developing Th2 cells, whereas T-bet, HLX and ROG mRNA was selectively expressed in developing Th1 cells.

Keywords: Th1/Th2 cells; Chromatin remodeling; Human Th2 gene locus

1. Introduction

CD4 helper T cell-dependent immune responses are controlled by the balance of antigen-specific Th1 and Th2 cells (Mosmann and Coffman, 1989; Reiner and Locksley, 1995; Seder and Paul, 1994). Th1 cells produce IFNγ and Th2 cells produce IL-4, IL-5 and IL-13. For Th2 cell differentiation, IL-4R-mediated signal transduction, including signal transducer and activator of transcription (STAT) 6 activation is required, while IL-12-mediated STAT4 activation plays an important role in Th1 cell differentiation (Constant and Bottomly, 1997; Gately et al., 1998; Murphy et al., 2000; Nelms et al., 1999; O'Garra, 1998). In addition to these cytokines, TCR-mediated signaling is also indispensable for Th1/Th2 cell differentiation (Constant and Bottomly, 1997). In particular, the fate of Th1/Th2 cell differentiation appears to be controlled by the TCR-mediated activation of the Ras/MAPK cascade (Shibata et al., 2002; Yamashita et al., 1999; Yamashita et al., 2005). Both c-Jun NH_2-terminal kinase (JNK) and the p38 MAPK cascade have also been reported to play an important role in Th1 cell differentiation and Th1 cytokine production (Dong et al., 1998; Rincon et al., 1998; Yang et al., 1998). The role for NF-κB activation in Th1/Th2 cell differentiation has also been suggested (Barnes and Karin, 1997; Das et al., 2001; Inami et al., 2004). Several transcription factors that control Th1/Th2 cell differentiation have been identified. Among them, GATA3 appears to be a key factor for

Corresponding author. Tel.: +81 43 226 2200; fax: +81 43 227 1498.
E-mail address: tnakayama@faculty.chiba-u.jp (T. Nakayama).

0161-5890/$ – see front matter © 2006 Elsevier Ltd. All rights reserved.
doi:10.1016/j.molimm.2006.11.004

Th2 cell differentiation (Lee et al., 2000; Ouyang et al., 1998; Zhang et al., 1997; Zheng and Flavell, 1997), and T-bet was recently identified to be a key transcription factor for Th1 cell differentiation (Szabo et al., 2000).

Changes in the chromatin structure, chromatin remodeling of the murine Th2 cytokine (IL-4/IL-5/IL-13) gene loci occur during Th2 cell differentiation (Ansel et al., 2006; Lee et al., 2006; Lohning et al., 2002). Various modifications of the N-terminal tail of histones play critical roles in the epigenetic regulation of transcription. Among them, the acetylation of lysine 9 of histone H3 (H3-K9) and the methylation of lysine 4 of histone H3 (H3-K4) are typically associated with the transcriptionally active regions of chromatin (Turner, 2002). We and others recently demonstrated that histone H3-K9 hyper-acetylation of the Th2 cytokine gene loci occurs in developing Th2 cells in a Th2-specific and STAT6/GATA3-dependent manner (Avni et al., 2002; Yamashita et al., 2002). In addition, the long-range histone hyper-acetylation regions within the IL-13/IL-4 and IL-5 gene loci in developing Th2 cells and Tc2 cells were revealed (Inami et al., 2004; Omori et al., 2003; Yamashita et al., 2002).

In human, the promoter region of the IFNγ gene locus was reported to be hypermetylated in Th2 cells but hypomethylated in Th1 cells (Yano et al., 2003). In addition, histone acetylation of the IFNγ gene locus was associated with Th1 cell differentiation (Morinobu et al., 2004). The induction of DNase I hypersensitive sites and CpG demethylation at the IL-4 and IL-13 gene loci occurred during human Th2 cell differentiation (Santangelo et al., 2002). Subsequently, histone H3-K9 hyper-acetylation at the IL-4 promoter region in human memory Th2 cells was reported (Messi et al., 2003). However, it has not been reported how histone modifications at the various Th2 cytokine gene loci occur in developing human Th2 cells. We herein established an *in vitro* Th1/Th2 cell differentiation system using peripheral blood human naïve CD4 T cells, and extensively investigated the histone modifications at the various regions within the Th2 cytokine gene loci. Our results indicate that histone H3-K9/14 hyper-acetylation and H3-K4 hyper-methylation occurred throughout the Th2 cytokine gene loci in human developing Th2 cells.

2. Materials and methods

2.1. Purification of naïve CD4 T cells and differentiation of the naïve CD4 T cells into Th1 and Th2 cells

The protocol was approved by the Institutional Ethics Committee, Graduate School of Medicine, Chiba University. Human PBMC were isolated from healthy volunteer by Ficoll-Paque density gradient centrifugation, and naïve CD4 T cells ($CD4^+$, $CD45RA^+$) were purified with human naïve CD4 T cell isolation kits (Mylteni Biotec Inc.) and an auto-MACS sorter. The purity ($CD4^+$, $CD45RA^+$) was more than 95% (Supplemental Figure 1). We used these cells for naïve T cells. For Th1 and Th2 cells, the enriched naïve CD4 T cells (1×10^6) were stimulated for 2 days with 20 μg/ml immobilized anti-CD3 mAb (Orthoclone OKT3 Injection, Raritan, NJ) in the presence of 3 μg/ml anti-CD28 mAb (BD-555725; Pharmingen), 50 units/ml IL-2 (Imunace 35, Shionogi & Co. Ltd., Osaka, Japan), 1 ng/ml IL-12 (no. 200-12; R&D systems), and 5 μg/ml anti-IL-4 mAb (BD-554481; Pharmingen) for Th1 culture conditions. For Th2 conditions, the cells were stimulated with 20 μg/ml immobilized anti-CD3 mAb in the presence of 3 μg/ml anti-CD28 mAb, 50 units/ml IL-2, 1 ng/ml IL-4 (no. 204-IL; R&D systems), and 5 μg/ml anti-IFNγ mAb (BD-554547; Pharmingen). The cells were then transferred to new plates, and cultured for another 5 days in the presence of cytokines and antibodies used in the original culture. Another cycle of the stimulation was performed. The cultured T cells were re-stimulated with 10 ng/ml phorbol myristate acetate (PMA) and 1 μM ionomycin for 4 h in the presence of 2 μM monensin. The Th1/Th2 cell differentiation was assessed by intracellular cytokine staining (Yamashita et al., 2002). Anti-IL-4 mAb (no. 340451; Becton Dickinson) and anti-IFNγ mAb (no. 340449; Becton Dickinson) were used.

2.2. ELISA

The cultured human Th1/Th2 cells were re-stimulated with 10 ng/ml PMA and 1 μM ionomycin in 48-well flat bottom plates for 24 h. The production of IL-2, IL-4, IL-5, IL-13 and IFNγ was measured by ELISA as previously described (Ishikawa et al., 2005; Shirai et al., 2003).

2.3. Chromatin immunoprecipitation (ChIP) assay

The ChIP assay was performed using histone H3 ChIP assay kits (no. 17-245; Upstate Biotechnology) with antibodies specific for acetylated histone H3 (at both lysine residues 9 and 14; upstate #06-599) and dimethylated histone H3 (at lysine residues 4; abcam ab7766) as described previously (Yamashita et al., 2002, 2006). In brief, 2×10^6 CD4 T cells were fixed with paraformaldehyde (1%) at 37 C for 15 min. The cells were sedimented, washed, lysed with a SDS lysis buffer (50 mM Tris–HCl, 1% SDS, 10 mM EDTA, 1 mM PMSF, 1 μg/ml aprotinin and 1 μg/ml pepstatin A). The lysates were sonicated to reduce DNA lengths to between 200 and 1000 bp. The soluble fraction was diluted, precleared with salmon sperm DNA/protein A agarose, and then incubated with antibody (5 μg/ml) specific for the acetylated and dimethylated forms of histones H3. Next, immune complexes were precipitated with protein A agarose. The precipitated DNA was eluted with an elution buffer (0.1 M $NaHCO_3$ containing 1% SDS). The eluted material was incubated at 65 C for 6 h to reverse the formaldehyde cross-links, and DNA was extracted with phenol and chloroform. Ethanol-precipitated DNA was solubilized in water (2×10^6 cell equivalent/100 μl). Semi-quantitative PCR was performed with 3 and 1 μg of DNA samples (a three-fold dilution) at 31 cycles. PCR products were resolved by agarose gel electrophoresis and visualized with ethidium bromide. The images were recorded and quantified using ATTO L&S analyzer (ATTO, Tokyo, Japan). Semi-quantitative PCR was performed using the primers listed in Supplemental Table 1.

2.4. Quantitative RT-PCR

Total RNA was isolated using TRIzol reagent (GIBCO BRL). Reverse transcription was done using Superscript II (Gibco-BRL). For quantitative real time PCR, a TaqMan universal PCR master mix was used for all reactions (Applied Biosystems), and the ABI Prism 7000 Sequence Detection System was employed (Kimura et al., 2005). The primers and TaqMan probes for the detection of human GATA3, T-bet, Eomesodermin, HLX, ROG and 18S were purchased from Applied Biosystems. The data are shown as the relative expression to the 18S signal.

3. Results

3.1. Histone H3-K9/14 hyper-acetylation and H3-K4 hyper-methylation at the Th2 cytokine gene loci in human Th2 cell

In order to examine the chromatin status of the human Th2 cytokine gene loci during the differentiation of naïve CD4 T cells into Th1 and Th2 cells, we established an *in vitro* differentiation system using freshly isolated human peripheral blood T cells. Naïve CD4 T cells ($CD4^+$, $CD45RA^+$) were cultured under Th1/Th2 culture conditions as described in the Materials and methods. The intracellular IFNγ/IL-4 profiles (Fig. 1A) and the levels of cytokine production (IL-4, IL-5, IL-13, and IFNγ) assessed by ELISA are shown (Fig. 1B). The developing Th2 cells produced substantial amounts of IL-4, IL-5 and IL-13 upon restimulation, and Th1 cells produced IFNγ selectively.

In order to examine the acetylation status of H3-K9/14 and the methylation status of H3-K4 in naïve CD4 T, *in vitro* differentiated Th1 and Th2 cells, we prepared a series of primer pairs throughout the Th2 cytokine gene loci (Fig. 1C). The ChIP assay was performed with antibodies specific for acetylated H3-K9/14 and dimethylated H3-K4. The real PCR bands (Fig. 1D) and the relative intensity of PCR bands (anti-acetyl H3-K9/14 or anti-dimethyl H3-K4/input DNA) are shown in Fig. 1E. The levels of histone H3-K9/14 acetylation associated with the Th2 cytokine gene loci (IL-5p, CGRE, IL-13p, CNS1, IL-13 intergenic, IL-4p, IL-4 exon 3, V_A enhancer, and CNS2 regions) were substantially higher in Th2 cells than in either naïve CD4 T or Th1 cells (Fig. 1E, left panel). In addition, the Th2-specific histone H3-K4 hyper-methylation at the Th2 cytokine gene loci (IL-5p, CGRE, IL-13p, CNS1, IL-13 intergenic, IL-4p, IL-4 exon 3, V_A enhancer, CNS2 and IL-4 intergenic regions) was observed (Fig. 1E, right panel). The acetylation of histone H3-K9/14 and methylation of histone H3-K4 at the RAD50 gene was equiva-

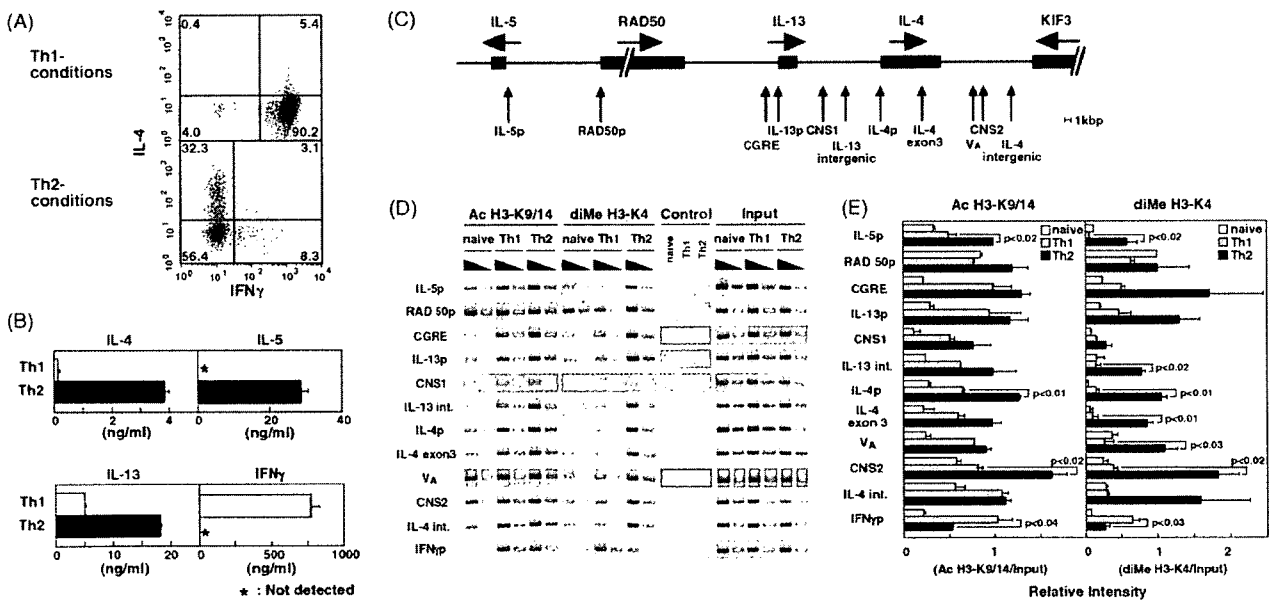

Fig. 1. Acetylation and methylation status of histone H3 at the Th2 cytokine gene loci. Human naïve CD4 T cells ($CD4^+$, $CD45RA^+$) purified from peripheral blood mononuclear cells were stimulated under Th1/Th2 conditions. (A) The levels of Th1/Th2 cell generation were assessed by intracellular cytokine staining. Representative IFNγ/IL-4 profiles are shown. (B) *In vitro* cultured Th1 and Th2 cells were stimulated with PMA and Ionomycin for 24 h, and the amounts of IL-4, IL-5, IL-13 and IFNγ in the culture supernatant were assessed by ELISA. The mean values with standard deviation of the triplicate cultures are shown. (C) Schematic representation of the human Th2 cytokine gene loci on chromosome 5q, and the locations of PCR primer pairs used in the ChIP assay are shown. (D) Acetylation status of histone H3-K9/14 and methylation status of H3-K4 at the Th2 cytokine gene loci. An isotype-matched control Ab (normal rabbit IgG, Santa Cruz sc-2027) was used. The ChIP assay was performed with naïve CD4T, Th1 and Th2 cells using the indicated primer pairs. Before immunoprecipitation, aliquots (6×10^2 cell equivalents) were removed for PCR to determine the relative levels of input DNA. To quantify the reactive levels of acetylation and methylation, a three-fold serial dilution was made with both the input DNA and immunoprecipitated DNA samples before PCR, and the PCR product intensities were then assessed. Three independent experiments with different T cell preparations were performed with similar results. (E) Quantitative representations of the bands measured at the highest concentration by densitometry, and the relative intensities (immunoprecipitates with anti-acetyl H3-K9 or anti-dimethyl H3-K4/input DNA) in each primer pair were calculated. The mean values with standard deviation are shown. The Student p values are shown where the difference is statistically significant.

lent in naïve CD4 T, Th1 and Th2 cells. As expected, increased histone H3-K9/14 hyper-acetylation and histone H3-K4 hyper-methylation on the IFNγ promoter region was preferentially observed in Th1 cells.

3.2. Histone H3-K9/14 hyper-acetylation and H3-K4 hyper-methylation around the IL-5 gene locus in developing Th2 cells

We previously reported that the intergenic region between the IL-5 and RAD50 gene locus was hyper-acetylated in a long range in mouse Th2 cells (Inami et al., 2004). No conserved GATA binding sequences between mouse and human was found around the downstream border of the long-rage acetylation region. This is in contrast to CGRE (conserved GATA3 response element) which existed in the upstream region of the IL-13 gene locus, and at the border of the long range hyperacetylation region within the IL-13 and IL-4 gene loci (Yamashita et al., 2002). Consequently, we more precisely examined the histone modifications at the intergenic region of IL-5 ad RAD50 by preparing a series of primer pairs between the IL-5 and RAD50 gene loci (Fig. 2A). A representative result of a ChIP assay of naïve CD4 T cells and *in vitro* differentiated Th1 and Th2 cells from a HV are shown in Fig. 2B. The relative band intensities (anti-acetyl H3-K9 or anti-dimethyl H3-K4/input DNA) of 19 primer pairs are depicted in Fig. 2C. The long-range Th2-specific histone H3-K9/14 hyper-acetylation and H3-K4 hyper-methylation were observed between the IL-5 and the RAD50 gene locus. Th1 cells showed a slightly increased acetylation as compared with that of naïve CD4 T cells, whereas no increased H3-K4 methylation was detected in Th1 cells.

3.3. Histone H3-K4 hyper-methylation in in vitro differentiated Th2 cells prepared from 20 healthy volunteers

In order to generalize the observation above, we next assessed the levels of histone H3-K4 methylation at the selected regions (IL-5 exon 3, IL-5p, IL-5 intergenic, RAD50p, CGRE, IL-13p, CNS1, IL-4p, V_A, and IFNγp) in developing Th1/Th2 cells prepared from 20 healthy volunteers (HV). The intracellular IFNγ/IL-4 profiles of the *in vitro* cultured developing Th1/Th2 cells from 20 HV are shown in Supplemental Figure 2. A ChIP assay using antibodies specific for dimethylated histone H3-K4 was performed. The real PCR bands are shown in Supplemental Figure 3, and the relative intensity (anti-dimethyl histone H3-K4/input DNA) is shown in Supplemental Figure 4. The mean values with standard deviations of the relative intensity for 20 HV are shown in Fig. 3B. The mean values of the methylated histones at the IL-5 exon 3, IL-5 promoter, IL-5 intergenic, CGRE, IL-13 promoter and IL-4 promoter regions were significantly higher in Th2 cells than those in Th1 cells. The levels of methylation of RAD50 promoter and CNS1 and V_A enhancer regions were not significantly different between Th1 and Th2 cells. The mean value of the methylated histones on IFNγ promoter was statistically higher in Th1 cells than in Th2 cells.

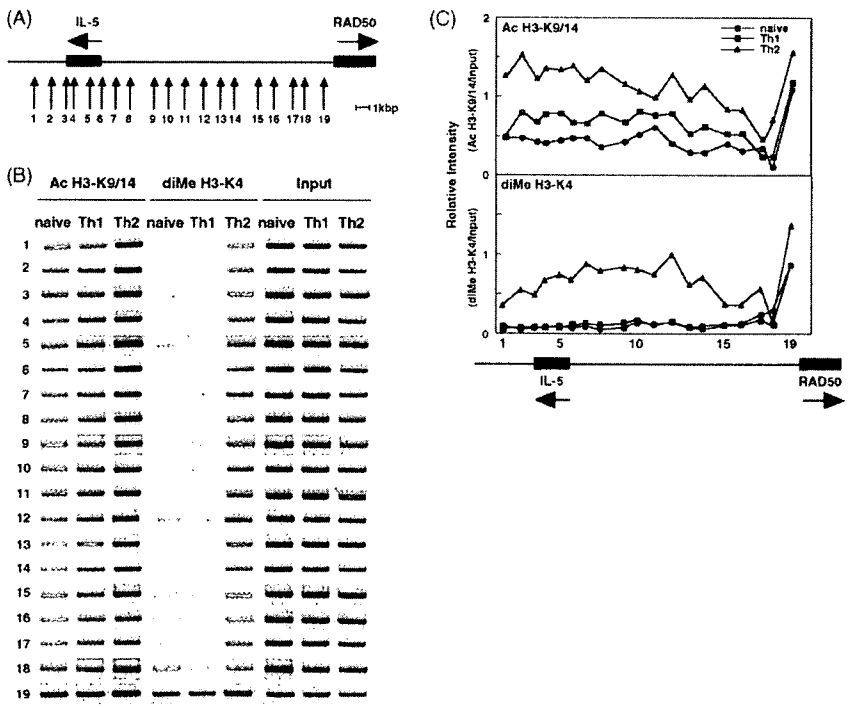

Fig. 2. Hyper-acetylation of histone H3-K9 and hyper-methylation of histone H3-K4 around the IL-5 and RAD50 loci in developing Th2 cells. (A) Schematic representation of the human IL-5 and RAD50 loci and the locations of PCR primer pairs used in the ChIP assay. (B) Naïve CD4 T, developing Th1 and Th2 cells were prepared and subjected to ChIP assays with the primer pairs indicated in (A). A representative result of a HV is shown. (C) The relative PCR band intensities (immunoprecipitates with anti-acetyl H3-K9 or anti-dimethyl H3-K4/input DNA) in each primer pair shown in panel B are shown.

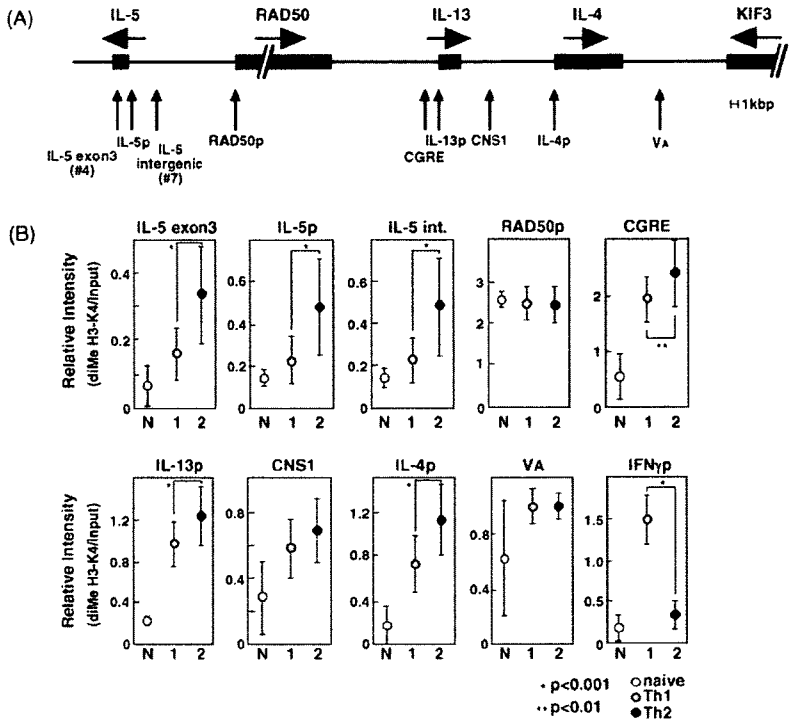

Fig. 3. Hyper-methylation of histone H3-K4 at the Th2 cytokine gene loci in *in vitro* differentiated Th2 cells. (A) A schematic representation of the Th2 cytokine gene loci and the locations of PCR primer pairs used in the ChIP assay. The primer named IL-5 exon 3 is the same as #4 primer used in Fig. 2. The primer named IL-5 intergenic is the same as #7 primer used in Fig. 2. (B) The methylation status of histone H3-K4 at the indicated region in naïve CD4T and *in vitro* differentiated Th1 and Th2 cells from 20 HV. ChIP assays with an anti-dimethyH3-K4 antibody, and the measurement of the relative intensities of the PCR bands were performed as described in Fig. 1. The mean values with standard deviation are shown. The student *p* values are shown in each panel.

3.4. mRNA expression levels of transcription factors that are preferentially expressed in Th1/Th2 cells

In a mouse system, the mRNA expression levels of various transcription factors (GATA3, T-bet, Eomesodermin, HLX, and ROG) are well documented to be involved in Th1/Th2 cell differentiation. Consequently, we wanted to examine the expression levels of these factors in our *in vitro* differentiated human Th1/Th2 cells. mRNA prepared from naïve and the *in vitro* cultured Th1 and Th2 cells from 20 HV were subjected to real time PCR analysis, and the relative expression (/18S) of the above transcription factors are shown in Fig. 4A. The mean values with standard deviations are shown in Fig. 4B. The expression levels of GATA3 mRNA were significantly higher in the developing Th2 cells than those of the developing Th1 cells. Whereas the mRNA expression levels of T-bet, HLX, and ROG were higher in the developing Th1 cells than in the Th2 cells. The levels of Eomesodermin were not statistically different between Th1 and Th2 cells. Moreover, the cytokine production data are shown in Fig. 4C. The results indicate that basically no IL-4, IL-5 or IFNγ was produced in naïve T cells, while there was a preferential induction of IL-4 and IL-5 in Th2 cells, and that of IFNγ in Th1 cells.

4. Discussion

In the present study, we established *in vitro* Th1/Th2 cell differentiation culture system using human peripheral blood naïve CD4 T cells. Using these *in vitro* developing Th1 and Th2 cells, we provide the first evidence indicating that in the human system, histone H3-K9/14 hyper-acetylation and H3-K4 hyper-methylation occurred throughout the Th2 cytokine gene loci in developing Th2 cells. Similar to mouse Th2 cells, chromatin remodeling of the intergenic region of the IL-5 and RAD50 gene loci was observed preferentially in Th2 cells.

The Th2 cytokine genes, IL-4, IL-5 and IL-13 are localized within a 125-kb region in the mouse and human (Mohrs et al., 2001). These cytokines are coordinately expressed in Th2 cells. We recently demonstrated that histone H3-K9 hyper-acetylation of the Th2 cytokine gene loci occurs in mouse Th2 cells in a Th2-specific and STAT6/GATA3-dependent manner (Yamashita et al., 2002). In addition, the long-range histone hyper-acetylation regions within the IL-13/IL-4 gene loci (Yamashita et al., 2002) were revealed in developing Th2 cells. The methylation of histone H3-K4 is also known to be an epigenetic marker typically associated with transcriptionally active chromatin (Milne et al., 2002; Nakamura et al., 2002). However, the methylation status of histone H3-K4 at the Th2 cytokine gene loci in human Th2 cells were not formally investigated. In the present study, we extensively investigated the histone H3-K4 methylation within the Th2 cytokine loci using 20 healthy volunteers' Th1/Th2 cell samples, and found that hyper-methylation occurs preferentially in the human developing Th2 cells (Figs. 1 and 3). Histone H3-K9 hyper-acetylation at the enhancer regions for Th2 cytokines (CNS1 and V_A enhancer) was preferentially detected in mouse Th2 cells (Yamashita et al., 2002). Interestingly, however, the

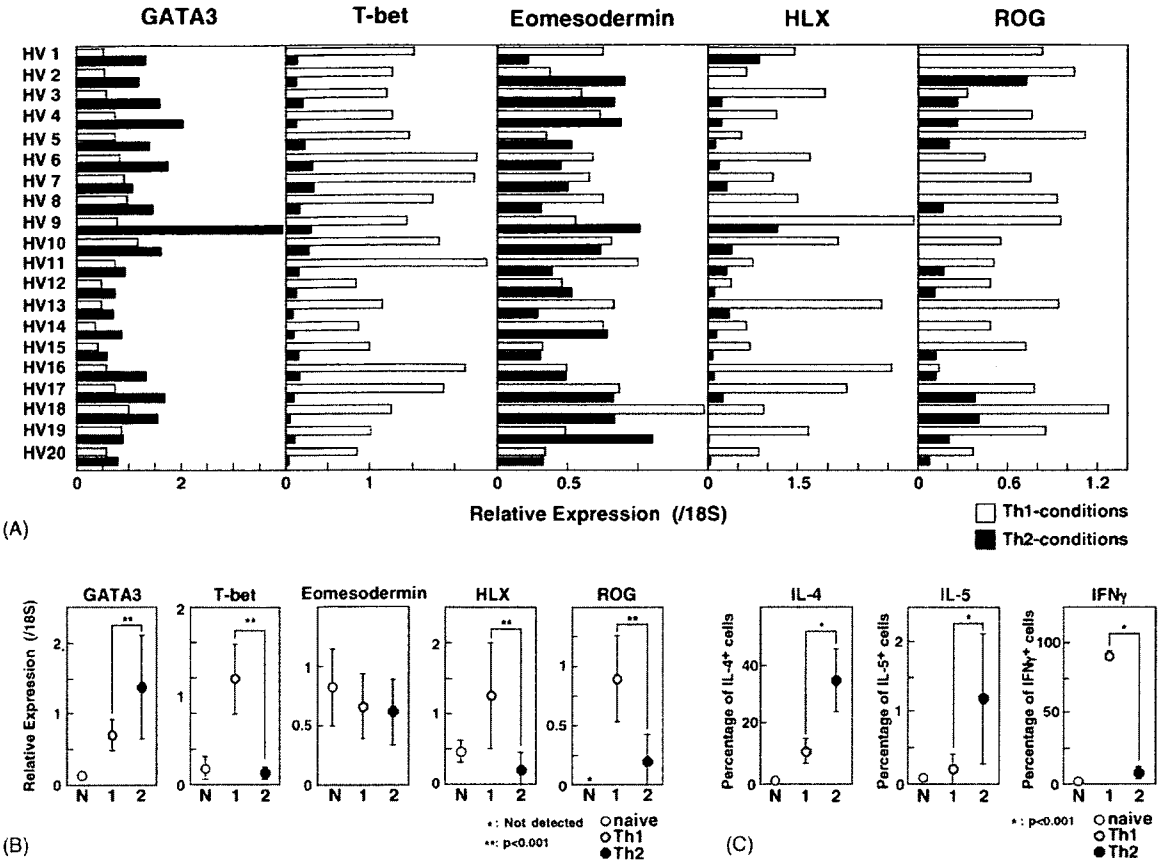

Fig. 4. mRNA expression levels of GATA3, T-bet, Eomesodermin, HLX and ROG in Th1 and Th2 cells. mRNA was prepared from *in vitro* cultured Th1 and Th2 cells from 20 HV, and real time quantitative PCR analysis was performed. (A) The relative expression (/18S) of the GATA3, T-bet, Eomesodermin, HLX, and ROG in Th1 and Th2 cells from 20 healthy volunteers are shown. (B) The mean values and standard deviations are shown. The Student p values are shown in each panel. (C) We performed cytoplasmic staining (IL-4, IL-5 and IFNγ) of naïve, Th1 and Th2 cells (20 HV), and the mean values and standard deviations are shown. The Student p values are shown in each panel.

levels of the methylation at CNS1 and V_A enhancer regions were not statistically higher in Th2 cells (Fig. 3). Although it is not clear at this time which molecules are responsible for this difference, one cause may be the difference in the increase in the expression of GATA3 between mouse and human Th2 cells. We detected more than a five-fold increase in GATA3 expression in mouse developing Th2 cells as compared with naïve CD4 T or Th1 cells (Omori et al., 2003), whereas the GATA3 expression in the developing human Th2 cells increased at most by about two-fold (Fig. 4). Since the binding affinity of GATA3 to the CNS1 and V_A enhancer regions were low in comparison to CGRE, another GATA3-binding motif critical for chromatin remodeling of the IL-4/IL-13 gene loci (Yamashita et al., 2002), chromatin remodeling of these regions (CNS1 and V_A enhancer) may not be efficiently induced.

More recently, we demonstrated a long-range histone hyper-acetylation with transcriptions within the IL-5 and the intergenic regions between the IL-5 and RAD50 genes (Inami et al., 2004). Similar to mouse Th2 cells, the present analysis revealed that the long-range histone hyper-acetylation of H3-K9/14 accompanied with hyper-methylation of histone H3-K4 occurred in human Th2 cells (Fig. 2). In addition, a relatively unmodified (hypo-acetylation) region was detected at 1600–1200 bp upstream of the RAD50 gene in Th2 cells (Fig. 2). Similar unmodified regions were observed in the mouse system (Inami et al., 2004). Therefore, similar molecular events may operate during the chromatin remodeling of the IL-5 gene locus in mouse and human developing Th2 cells.

As we expected, the expression levels of GATA3 were significantly higher in Th2 cells, while those of T-bet were higher in Th1 cells (Fig. 4). HLX is a Th1-restricted homeobox transcription factor, which appears to interact with T-bet to achieve the induction of an optimal expression of IFNγ in mouse Th1 cells (Mullen et al., 2002). ROG is a POZ (BTB) domain-containing zinc finger repressor, and the expression levels of ROG mRNA were significantly higher in the mouse developing Th1 cells than in Th2 cells (Omori et al., 2003). Similar to the mouse system, we observed an increased expression of HLX and ROG in human Th1 cells using 20 healthy volunteers' Th1/Th2 cells (Fig. 4). Eomesodermin is induced in mouse effector CD8 T cells, and it is necessary for the full effector differentiation of CD8 T cells, including the acquisition of a sufficient IFNγ expression. The expression of Eomesodermin is restricted to CD8 T cells (Pearce et al., 2003). We detected a low level expression of Eomesoder-